Article

Journal of Vibration and Control
18(2) 246–267

DOI: 10.1177/1077546311402530
jvc.sagepub.com

Exact analytical solution for free vibration of functionally graded thin annular sector plates resting on elastic foundation

A Hasani Baferani, AR Saidi and E Jomehzadeh

Abstract

This article introduces an exact analytical method for free vibration analysis of functionally graded (FG) thin annular sector plates resting on Winkler and Pasternak elastic foundations. The annular sector plate has simply supported radial edges and arbitrary boundary conditions along the circular edges. Based on the displacement field of Kirchhoff plate theory, the governing equations of motion are obtained considering the in-plane displacements and rotary inertia. Using a set of functions, the three coupled governing equations of motion are converted into two decoupled equations. By applying the boundary conditions at inner and outer radii, an eigenvalue problem for finding the natural frequencies is obtained. The nine distinct cases are considered involve all possible combinations of boundary conditions along the circular edges. Accurate non-dimensional frequency is presented for over a wide range of sector angles, some inner to outer radii (aspect ratio) and different powers of functionally graded material. Accurate natural frequencies of FG annular sector plates resting on elastic foundations are presented for the first time and can be used as reference values for numerical analyses.

Keywords

Elastic foundation, free vibration, functionally graded, thin annular sector plate

Received: 4 July 2010; accepted: 27 December 2010

1. Introduction

Many problems of considerable practical importance can be related to the solution of plates resting on elastic foundations. Reinforced concrete pavement foundation slabs of buildings are the well-known direct applications of plates on an elastic foundation.

Generally, the analysis of structures on the elastic foundation is developed on the assumption that the reaction forces of the foundation are proportional at every point to the deflection of the structure at that point.

The functionally graded materials (FGMs) are newly discovered materials which are used, because of their remarkable mechanical properties, in many engineering applications namely space structures, aerospace and other industries. The mechanical properties of FGMs vary smoothly and continuously from one surface to the other (Shiota and Miyamoto, 1997). These materials are usually made from a mixture of metal and ceramic, or a combination of different metals.

There are lots of studies for free vibration analysis of homogenous annular sector plates in the literature. Cheung and Kwok (1975) studied the dynamic analysis of circular and sector thick, layered plates by using the finite element method. Srinivasan and Thiruvekatachari (1986) by using an integral equation technique studied the free vibration analysis of laminated annular sector plates. By using the Rayleigh-Ritz method, Kim and Dickinson (1989) investigated the free vibration of annular and circular thin plates subject to certain complicating effects. Harik and Molaghasemi (1990) employed an analytical method to investigate the free vibration of isotropic annular sector plates resting on

Department of Mechanical Engineering, Shahid Bahonar University of Kerman, Iran

Corresponding author:
AR Saidi, Department of Mechanical Engineering, Shahid Bahonar University of Kerman, Kerman, Iran
Email: saidi@mail.uk.ac.ir

elastic foundations. By using the spline element method, Mizusawa (1991) presented the free vibration of stepped annular sector plates. He concluded that the frequencies of the annular stepped sector plates are influenced by the sector angles, the stepped width ratios and the stepped thickness ratios. By using the Rayleigh-Ritz procedure, Xiang et al. (1993) investigated the free vibration of thick sector plates with different supporting edge conditions. McGee et al. (1993, 1995) presented the comprehensive exact solutions for free vibration of thick annular sectorial plates with simply supported radial edges. They presented exact results for homogenous isotropic annular sector plates under different boundary conditions. Based on Mindlin theory, Huang et al. (1994) presented exact analytical solutions for free vibrations of thick sectorial plates with simply supported radial edges. Huang and Ho (2004) studied the analytical solution for free vibrations of a polarly orthotropic Mindlin sectorial plate with simply supported radial edges, by using the Frobenius method. Also by using the Ritz method and considering stress singularities, Huang et al. (2006) studied the vibrations of Mindlin sectorial plates. Wang and Wang (2004) studied the free vibration analysis of thin sector plates by a new version of differential quadrature method. Seok and Tiersten (2004a,b) investigated the free vibration of annular sector cantilever plates for in-plane and out of plane motion, respectively. Yongqiang and Jian (2007) investigated the free vibration analysis of circular and annular sectorial thin plates using curve strip Fourier p-element. Zhou et al. (2009) studied the three dimensional vibration analysis of annular sector plates using the Chebyshev–Ritz method. Based on the First order shear deformation theory, Jomehzadeh and Saidi (2009a,b) presented an analytical solution for free vibration of transversely isotropic of complete sector and annular sector plates. Malekzadeh (2009) investigated three-dimensional free vibration analysis of thick laminated annular sector plates using a hybrid method.

Although many studies have been carried out for vibration analysis of homogenous sector plate, a little article can be found on vibration of functionally graded (FG) sector plates. Nie and Zhong (2008) presented the free and forced vibration analysis of FG annular sectorial plates with simply supported radial edges by using the differential quadrature method. They concluded that the lowest non-dimensional frequency decreases with the increase of the FG index for different thickness ratios, radii ratios and sector angles and it increases with the increase of thickness ratios, radii ratios and the circumferential wave number. Hosseini-Hashemi et al. (2010a) studied the buckling and free vibration behaviors of radially FG circular and annular sector thin plates subjected to uniform in-plane compressive loads and resting on the Pasternak elastic foundation. In the case of radially FGM, the bending and stretching equations are decoupled and the plate equations can be solved like the homogenous ones. Since the FG plates are usually used where there is a temperature difference in thickness direction, the material properties of FG plate should vary through the thickness in which the bending/stretching equations become coupled and finding the analytical solution is difficult in this case. Malekzadeh et al. (2010b) presented dynamic response of thick laminated annular sector plates subjected to moving load by using the finite difference method. Malekzadeh et al. (2010a) studied the three-dimensional layer–wise finite element free vibration analysis of thick laminated annular plates on elastic foundation. Hosseini-Hashemi et al. (2010b) presented the vibration analysis of radially FG sectorial plates of variable thickness on elastic foundations by using the differential quadratic method.

To the best of the authors' knowledge, the analytical solutions for the free vibration of FG annular sector plates have not been presented in the literature, yet.

The object of the present article is to give an exact solution for free vibration analysis of FG sector plates resting on an elastic foundation. The properties of material are assumed to vary through the thickness that makes the problem more complicated. The governing equations of motion are obtained using the Hamilton's principle. Three coupled bending/stretching equations of motion are decoupled and solved by using two auxiliary functions. For solving the decoupled equations, it is assumed that the FG annular sector plate has simply supported radial edges and arbitrary boundary conditions along the circular edges. The non-dimensional frequencies are tabulated for FG sector plates with all nine different boundary conditions along the circular edges. Finally, the effects of sector angle, thickness-radius ratio, aspect ratio, material properties and elastic foundation coefficients on the vibration behavior of FG annular sector plate are studied in details. The presented results for natural frequencies of FG annular sectorial plates are given for the first time and can serve as reference values for numerical analyses.

2. Elastic foundation

Many practical engineering problems can be related to the solution of plates resting on an elastic foundation. There exist various hypotheses models of elastic foundation of which two simple models are Winkler and Pasternak elastic foundations. Physically, the Winkler model (Winkler, 1867) can be considered as an idealization of the soil medium by a number of mutually independent spring elements. To account the more

realistic interaction between the springs, two-parameter models such as the Pasternak model (Pasternak, 1954) which permit interaction among the springs were proposed.

For accounting the Winkler foundation, it is assumed that the foundation's reaction $q(r,\theta)$ can be describe by the following mathematical relation

$$q(r,\theta) = K_w\, w(r,\theta) \tag{1}$$

where $w(r,\theta)$ is the deflection and K_w is Winkler elastic foundation parameter.

Also, for Pasternak model, the foundation's reaction is (Civalek, 2007)

$$q(r,\theta) = K_w\, w(r,\theta) + K_s\, \nabla^2 w(r,\theta) \tag{2}$$

where K_s is the interaction parameter of Pasternak foundation. Physically, these parameters represent the interaction due to shear action among the spring elements.

The physical difference between the Winkler and the Pasternak foundations may be observed from a circular plate with free edges under a transverse uniform load. The plate will undergo a uniform rigid body settlement when it rests on the former foundation whereas a "dishing" type of deflection occurs with the latter kind of foundation model.

3. Basic equations

Consider an FG annular sector plate with inner radius a, outer radius b, uniform thickness h and sector angle α (Figure 1). It is assumed that the annular sector plate is made of a mixture of ceramic and metal. Also, the Young modulus and mass density of the annular sector plate vary through the thickness as a power law, i.e.

$$\begin{aligned} E(z) &= E_m + (E_c - E_m)\left(\frac{1}{2} - \frac{z}{h}\right)^n \\ \rho(z) &= \rho_m + (\rho_c - \rho_m)\left(\frac{1}{2} - \frac{z}{h}\right)^n \end{aligned} \tag{3}$$

where n is the power of the FG plate. Also, E_m and E_c refer to Young modulus of metal and ceramic, respectively. According to the small range of Poisson ratio variation, it is assumed that it is constant through the thickness of the FG annular sector plate.

For a thin sector plate, the displacement field is assumed as

$$u_r(r,\theta,z,t) = u(r,\theta,t) - z\frac{\partial w(r,\theta,t)}{\partial r} \tag{4a}$$

$$u_\theta(r,\theta,z,t) = v(r,\theta,t) - \frac{z}{r}\frac{\partial w(r,\theta,t)}{\partial \theta} \tag{4b}$$

$$w(r,\theta,z,t) = w(r,\theta,t) \tag{4c}$$

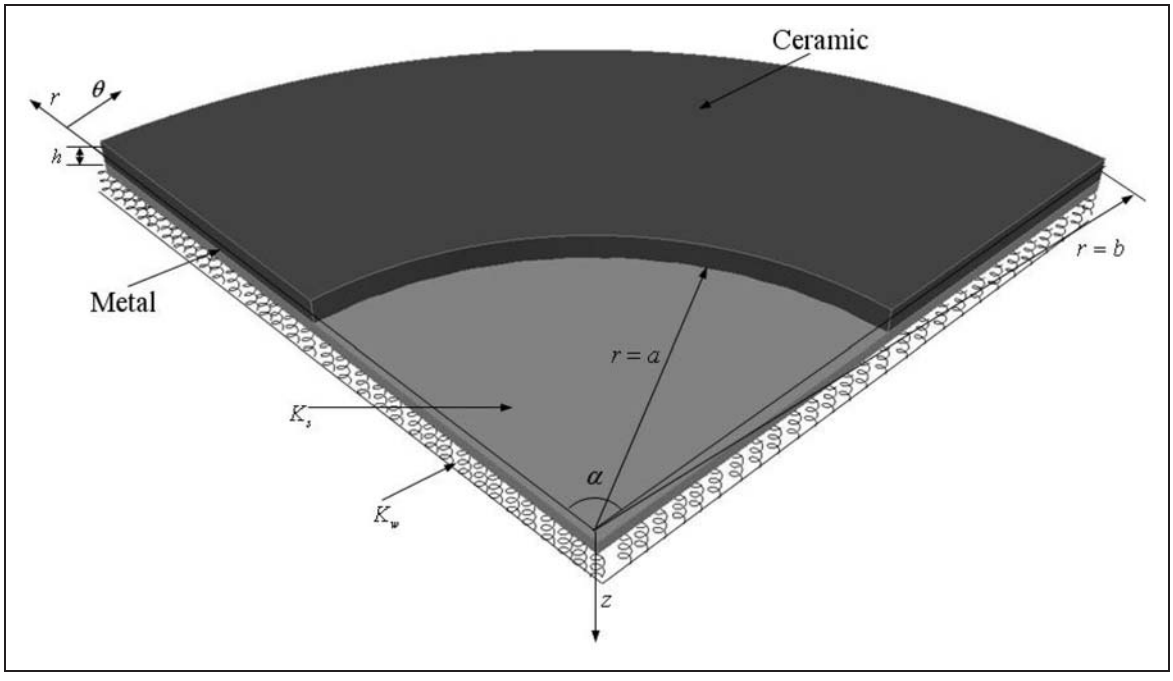

Figure 1. Geometry and coordinate system of an annular sector plate.

Table 1. Comparison of the natural frequency of annular sector plate, $\varpi_{mk} = \omega_{mk} b^2 \sqrt{\frac{\rho_m h}{D_m}}$ for all boundary conditions ($h/b = 0.001$, $\alpha = 195^\circ$)

		$a/b = 0.1$	$a/b = 0.3$	$a/b = 0.5$	$a/b = 0.7$
SSCC	3-D - Zhou et al. 2009	–	–	90.1125	–
	Mindlin-McGee et al. 1995	28.6308	46.4445	90.0837	249.051
	Present	28.6308	46.4447	90.0838	249.050
SSCS	3-D - Zhou et al. 2009	–	–	–	–
	Mindlin-McGee et al. 1995	19.11578	31.1848	60.8128	169.346
	Present	19.1157	31.18496	60.81283	169.34556
SSCF	3-D - Zhou et al. 2009	–	–	–	–
	Mindlin-McGee et al. 1995	3.5409	6.5485	13.2435	37.4161
	Present	3.54115	6.54861	13.24361	37.41634
SSSC	3-D - Zhou et al. 2009	–	–	–	–
	Mindlin-McGee et al. 1995	24.8439	35.5832	65.2605	175.352
	Present	24.84421	35.58331	65.26041	175.3509
SSSS	3-D - Zhou et al. 2009	–	–	41.5301	–
	Mindlin-McGee et al. 1995	16.3785	22.9819	41.5375	111.239
	Present	16.37863	22.98210	41.53744	111.2388
SSSF	3-D - Zhou et al. 2009	–	–	–	–
	Mindlin-McGee et al. 1995	2.5006	3.3374	4.7369	8.0567
	Present	2.50087	3.33758	4.73706	8.05680
SSFC	3-D - Zhou et al. 2009	–	–	21.4074	–
	Mindlin-McGee et al. 1995	20.4360	18.6384	21.4263	45.0122
	Present	20.43628	18.63861	21.42632	45.01249
SSFS	3-D - Zhou et al. 2009	–	–	10.8522	–
	Mindlin-McGee et al. 1995	13.2448	12.0356	10.8761	12.5616
	Present	13.24493	12.03580	10.87624	12.56188
SSFF	3-D - Zhou et al. 2009	–	–	0.1856	–
	Mindlin-McGee et al. 1995	0.3442	0.2413	0.1850	0.1462
	Present	0.34433	0.241562	0.185384	0.14639

Table 2. Comparison of the natural frequency (Hz) of annular sector plate with the results of ANSYS software ($b = 1$ *m*, $h = 0.05$ *m*, $\bar{K}_w = 0$, $\bar{K}_s = 0$)

		$a/b = 0.3$			$a/b = 0.5$		
α	Boundary condition	ANSYS	Present	Difference	ANSYS	Present	Difference
90°	*SSCC*	1199.60	1227.09	2.29%	2178.10	2234.31	2.58%
	SSCF	186.84	191.58	2.53%	346.71	354.10	2.13%
	SSFC	766.97	782.70	2.05%	744.63	772.11	3.69%
180°	*SSCC*	1109.10	1120.08	0.98%	2091.10	2161.50	3.36%
	SSCF	156.82	157.82	0.63%	317.74	320.18	0.77%
	SSFC	458.26	467.13	1.93%	520.75	529.85	1.74%
270°	*SSCC*	1089.40	1102.60	1.21%	2078.90	2148.60	3.35%
	SSCF	158.19	158.35	0.10%	315.23	316.31	0.34%
	SSFC	372.38	379.49	1.90%	471.89	482.03	2.14%

Table 3. Fundamental frequency parameter $\varpi_{mk} = \omega_{mk} b^2 \sqrt{\frac{\rho_m h}{D_m}}$ of *SSCC* FG annular sector plate for some values of n, α, $\bar{K}_w$, $\bar{K}_s$ and a/b ($h/b = 0.05$)

α	a/b	$(\bar{K}_w, \bar{K}_s)$	$n = 0$	$n = 0.5$	$n = 1$	$n = 2$	$n = 5$
$\frac{\pi}{3}$	1×10^{-6}	(0,0)	99.8879	84.5733	76.1855	69.2329	65.6266
		(10,10)	108.2673	92.1786	83.7209	76.7626	72.5372
	0.3	(0,0)	117.4868	99.4736	89.6067	81.42754	77.1851
		(10,10)	125.0020	106.2991	96.3762	89.5335	83.3973
	0.5	(0,0)	193.2422	163.6086	147.3621	133.8848	126.8958
		(10,10)	199.6286	169.4148	153.1291	139.6624	132.1924
$\frac{\pi}{2}$	1×10^{-6}	(0,0)	68.3768	57.8950	52.1584	47.4061	44.9407
		(10,10)	76.4234	65.1903	59.3757	54.6067	51.5537
	0.3	(0,0)	100.2056	84.8438	76.4343	69.4665	65.8518
		(10,10)	106.7751	90.8099	82.3512	75.3850	71.2822
	0.5	(0,0)	182.4571	154.4799	139.1482	126.4343	119.8405
		(10,10)	188.3183	159.8089	144.4418	131.7381	124.7031
$\frac{2\pi}{3}$	1×10^{-6}	(0,0)	54.4381	46.0936	41.5282	37.7472	35.7854
		(10,10)	62.2488	53.1694	48.5204	44.7149	42.1877
	0.3	(0,0)	94.9127	80.3630	72.3997	65.8027	62.3803
		(10,10)	101.0057	85.8965	77.8878	71.2928	67.4177
	0.5	(0,0)	178.9365	151.500	136.4670	124.0023	117.5374
		(10,10)	184.5901	156.6404	141.5733	129.1189	122.2285
π	1×10^{-6}	(0,0)	42.9562	36.3721	32.7708	29.7891	28.2419
		(10,10)	50.2392	42.9649	39.2789	36.2673	34.1969
	0.3	(0,0)	91.4678	77.4466	69.7738	63.4182	60.1209
		(10,10)	97.1616	82.6179	74.9030	68.5498	64.8293
	0.5	(0,0)	176.5110	149.4472	134.6199	122.3268	115.9509
		(10,10)	182.0082	154.4453	139.5851	127.3023	120.5126
$\frac{3\pi}{2}$	1×10^{-6}	(0,0)	43.3790	36.7303	33.0944	30.0843	28.5223
		(10,10)	49.3109	42.1050	38.4072	35.3802	33.3884
	0.3	(0,0)	90.0398	76.2377	68.6853	62.4299	59.1844
		(10,10)	95.5391	81.2325	73.6397	67.3868	63.7325
	0.5	(0,0)	175.4581	148.5559	133.8180	121.5995	115.2622
		(10,10)	180.8834	153.4888	138.7185	126.5102	119.7645
2π	1×10^{-6}	(0,0)	43.9409	37.2061	33.5233	30.4746	28.8925
		(10,10)	49.4088	42.1619	38.4240	35.3618	33.3823
	0.3	(0,0)	89.5562	75.8283	68.3166	62.0951	58.8672
		(10,10)	94.9848	80.7589	73.2075	66.9886	63.3572
	0.5	(0,0)	175.0932	148.2471	133.5401	121.3475	115.0236
		(10,10)	180.4931	153.1567	138.4177	126.2352	119.5048

where u, v and w are the mid-plane displacement components in r, θ and z directions, respectively.

For vibration analysis of homogeneous isotropic plates, neglecting the in-plane displacements does not have any effect on the natural frequencies because the stretching and bending equations are decoupled from each other. However, in the analysis of FG plate based on the coupling between bending and stretching equations the in-plane displacements are the major parameters. Therefore, in this article the effects of in-plane displacement are considered. Also, the effects of in-plane displacements are considered in detail in Hasani Baferani et al. (2010).

Under the assumption of small deformation and linear strain-displacement relations, the strain components of a FG annular sector plate can be

Table 4. Fundamental frequency parameter $\varpi_{mk} = \omega_{mk} b^2 \sqrt{\frac{\rho_m h}{D_m}}$ of *SSSC* FG annular sector plate for some values of n, α, $\bar{K}_w$, $\bar{K}_s$ and a/b ($h/b = 0.05$)

α	a/b	$(\bar{K}_w, \bar{K}_s)$	$n = 0$	$n = 0.5$	$n = 1$	$n = 2$	$n = 5$
$\frac{\pi}{3}$	1×10^{-6}	(0,0)	99.8879	84.5733	76.1855	69.2329	65.6266
		(10,10)	108.2673	92.1786	83.7209	76.7626	72.5372
	0.3	(0,0)	106.8757	90.4895	81.5140	74.0739	70.2148
		(10,10)	115.0137	97.8776	88.8370	81.3943	76.9322
	0.5	(0,0)	152.7616	129.3364	116.4955	105.8445	100.3210
		(10,10)	160.4401	136.3133	123.4191	112.7741	106.6761
$\frac{\pi}{2}$	1×10^{-6}	(0,0)	68.3768	57.8950	52.1584	47.4061	44.9407
		(10,10)	76.4234	65.1903	59.3757	54.6067	51.5537
	0.3	(0,0)	83.7409	70.9034	63.8761	58.0538	55.0334
		(10,10)	91.2699	77.7355	70.6439	64.8150	61.2397
	0.5	(0,0)	137.1715	116.1390	104.6148	95.0595	90.1037
		(10,10)	144.4577	122.7587	111.1833	101.6332	96.1331
$\frac{2\pi}{3}$	1×10^{-6}	(0,0)	54.4381	46.0936	41.5282	37.7472	35.7854
		(10,10)	62.2488	53.1694	48.5204	44.7149	42.1877
	0.3	(0,0)	75.8626	64.2333	57.8689	52.5969	49.8617
		(10,10)	83.0239	70.7308	64.3040	59.0244	55.7624
	0.5	(0,0)	131.8727	111.6533	100.5765	91.3932	86.6302
		(10,10)	138.9888	118.1182	106.9912	97.8129	92.5186
π	1×10^{-6}	(0,0)	42.9562	36.3721	32.7708	29.7891	28.2419
		(10,10)	50.2392	42.9649	39.2789	36.2673	34.1969
	0.3	(0,0)	70.4235	59.6284	53.7215	48.8291	46.2908
		(10,10)	77.2381	65.8108	59.8438	54.9435	51.9045
	0.5	(0,0)	128.1507	108.5024	97.7397	88.8178	84.1901
		(10,10)	135.1326	114.8454	104.0333	95.1161	89.9673
$\frac{3\pi}{2}$	1×10^{-6}	(0,0)	43.3790	36.7303	33.0944	30.0843	28.5223
		(10,10)	49.3109	42.1050	38.4072	35.3802	33.3884
	0.3	(0,0)	68.0796	57.6440	51.9342	47.2053	44.7518
		(10,10)	74.7110	63.6600	57.8915	53.1548	50.2142
	0.5	(0,0)	126.5152	107.1179	96.4932	87.6860	83.1178
		(10,10)	133.4337	113.4032	102.7294	93.9269	88.8425
2π	1×10^{-6}	(0,0)	43.9409	37.2061	33.5233	30.4746	28.8925
		(10,10)	49.4088	42.1619	38.4240	35.3618	33.3823
	0.3	(0,0)	67.2723	56.9605	51.3186	46.6460	44.2217
		(10,10)	73.8347	62.9138	57.2138	52.5334	49.6272
	0.5	(0,0)	125.9456	106.6357	96.0591	87.2918	82.7444
		(10,10)	132.8413	112.9003	102.2748	93.5122	88.4502

expressed as

$$\varepsilon_{rr} = \frac{\partial u}{\partial r} - z\left(\frac{\partial^2 w}{\partial^2 r}\right)$$

$$\varepsilon_{\theta\theta} = \frac{1}{r}\frac{\partial v}{\partial \theta} + \frac{u}{r} - z\left(\frac{1}{r^2}\frac{\partial^2 w}{\partial^2 \theta} + \frac{1}{r}\frac{\partial w}{\partial r}\right) \quad (5)$$

$$2\varepsilon_{r\theta} = \frac{1}{r}\frac{\partial u}{\partial \theta} + \frac{\partial v}{\partial r} - \frac{v}{r} - z\left(\frac{2}{r}\frac{\partial^2 w}{\partial r \partial \theta} - \frac{2}{r^2}\frac{\partial w}{\partial \theta}\right)$$

In the classical plate theory, it is assumed that the cross section perpendicular to the middle surface of the plate remains normal and unscratched after deformation.

Table 5. Fundamental frequency parameter $\varpi_{mk} = \omega_{mk} b^2 \sqrt{\frac{\rho_m h}{D_m}}$ of *SSCS* FG annular sector plate for some values of n, α, $\bar{K}_w$, $\bar{K}_s$ and a/b ($h/b = 0.05$)

α	a/b	$(\bar{K}_w, \bar{K}_s)$	$n = 0$	$n = 0.5$	$n = 1$	$n = 2$	$n = 5$
$\frac{\pi}{3}$	1×10^{-6}	(0,0)	78.2450	66.2492	59.6803	54.2362	51.4123
		(10,10)	87.8753	74.9803	68.3177	62.8527	59.3250
	0.3	(0,0)	88.9937	75.3496	67.8771	61.6835	58.4709
		(10,10)	98.0826	83.5947	76.0406	69.8345	65.9536
	0.5	(0,0)	138.9518	117.6445	105.9651	96.2779	91.2542
		(10,10)	147.2111	125.1467	113.4067	103.7223	98.0826
$\frac{\pi}{2}$	1×10^{-6}	(0,0)	50.2307	42.5309	38.3174	34.8274	33.0167
		(10,10)	59.8038	51.1941	46.8653	43.3315	40.8347
	0.3	(0,0)	71.0352	60.1456	54.1849	49.2466	46.6847
		(10,10)	79.4850	67.8066	61.7642	56.8083	53.6292
	0.5	(0,0)	126.4074	107.0252	96.4054	87.5999	83.0329
		(10,10)	134.2578	114.1554	103.4770	94.6735	89.5219
$\frac{2\pi}{3}$	1×10^{-6}	(0,0)	38.1098	32.2683	29.0727	26.4265	25.0535
		(10,10)	47.6335	40.8743	37.5466	34.8389	32.7933
	0.3	(0,0)	65.3493	55.3317	49.8494	45.3082	42.9521
		(10,10)	73.4202	62.6478	57.0857	52.5258	49.5814
	0.5	(0,0)	122.2376	103.4954	93.2276	84.7149	80.2997
		(10,10)	129.9135	110.4666	100.1414	91.6305	86.6440
π	1×10^{-6}	(0,0)	28.2498	23.9199	21.5518	19.5913	18.5740
		(10,10)	37.4742	32.2412	29.7258	27.6860	26.0282
	0.3	(0,0)	61.5905	52.1494	46.9833	42.7044	40.4844
		(10,10)	69.3164	59.1519	53.9083	49.6105	46.8281
	0.5	(0,0)	119.3413	101.0435	91.0203	82.7110	78.4011
		(10,10)	126.8806	107.8906	97.8107	89.5031	84.6323
$\frac{3\pi}{2}$	1×10^{-6}	(0,0)	28.3087	23.9699	21.5973	19.6331	18.6138
		(10,10)	36.2374	31.1274	28.6352	26.6101	25.0367
	0.3	(0,0)	60.0184	50.8183	45.7845	41.6153	39.4522
		(10,10)	67.5672	57.6601	52.5502	48.3621	45.6498
	0.5	(0,0)	118.0776	99.9737	90.0571	81.8366	77.5726
		(10,10)	125.5529	106.7627	96.7898	88.5708	83.7508
2π	1×10^{-6}	(0,0)	28.6560	24.2640	21.8623	19.8742	18.8425
		(10,10)	36.1299	31.0126	28.5004	26.4570	24.9018
	0.3	(0,0)	59.4840	50.3659	45.3770	41.2452	39.1014
		(10,10)	66.9671	57.1481	52.0836	47.9329	45.2448
	0.5	(0,0)	117.6389	99.6023	89.7228	81.5330	77.2851
		(10,10)	125.0913	106.3704	96.4348	88.2465	83.4443

Consequently, the transverse shear deformations are neglected. Substituting strain components (5) into the Hamilton's principle, the equations of motion of the FG sector plate resting on the Winkler and Pasternak elastic foundation are obtained as follows

$$\frac{\partial N_{rr}}{\partial r} + \frac{1}{r}\frac{\partial N_{r\theta}}{\partial \theta} + \frac{1}{r}(N_{rr} - N_{\theta\theta}) = I_0 \ddot{u} - I_1 \frac{\partial \ddot{w}}{\partial r} \tag{6a}$$

$$\frac{\partial N_{r\theta}}{\partial r} + \frac{2}{r} N_{r\theta} + \frac{1}{r}\frac{\partial N_{\theta\theta}}{\partial \theta} = I_0 \ddot{v} - I_1 \frac{\partial \ddot{w}}{r \partial \theta} \tag{6b}$$

$$\begin{aligned} &\frac{\partial^2 M_{rr}}{\partial r^2} + \frac{2}{r}\frac{\partial M_{rr}}{\partial r} + \frac{1}{r^2}\frac{\partial^2 M_{\theta\theta}}{\partial \theta^2} - \frac{1}{r}\frac{\partial M_{\theta\theta}}{\partial r} \\ &\quad + \frac{2}{r}\frac{\partial^2 M_{r\theta}}{\partial r \partial \theta} + \frac{2}{r^2}\frac{\partial M_{r\theta}}{\partial \theta} - K_w w + K_s\left(\frac{\partial^2 w}{\partial r^2} + \frac{\partial w}{r \partial r} + \frac{\partial^2 w}{r^2 \partial \theta^2}\right) \\ &\quad = I_0 \ddot{w} + I_1\left(\frac{\partial \ddot{u}}{\partial r} + \frac{\ddot{u}}{r} + \frac{1}{r}\frac{\partial \ddot{v}}{\partial \theta}\right) - I_2\left(\frac{\partial^2 \ddot{w}}{\partial r^2} + \frac{\partial \ddot{w}}{r \partial r} + \frac{\partial^2 \ddot{w}}{r^2 \partial \theta^2}\right) \end{aligned} \tag{6c}$$

Table 6. Fundamental frequency parameter $\varpi_{mk} = \omega_{mk} b^2 \sqrt{\frac{\rho_m h}{D_m}}$ of SSSS FG annular sector plate for some values of n, α, $\bar{K}_w$, $\bar{K}_s$ and a/b ($h/b = 0.05$)

α	a/b	$(\bar{K}_w, \bar{K}_s)$	$n = 0$	$n = 0.5$	$n = 1$	$n = 2$	$n = 5$
$\frac{\pi}{3}$	1×10^{-6}	(0,0)	78.2450	66.2492	59.6803	54.2362	51.4122
		(10,10)	87.8753	74.9803	68.3177	62.8528	59.3250
	0.3	(0,0)	82.0552	69.4751	62.5856	56.8756	53.9138
		(10,10)	91.5946	78.1255	76.5367	65.4175	61.7570
	0.5	(0,0)	109.4061	92.6304	83.4374	75.8140	71.8604
		(10,10)	118.8973	101.2447	91.9722	84.3416	79.6861
$\frac{\pi}{2}$	1×10^{-6}	(0,0)	50.2308	42.5309	38.3174	34.8274	33.0167
		(10,10)	59.8038	51.1942	46.8653	43.3315	40.8346
	0.3	(0,0)	59.3475	50.2498	45.2705	41.1456	39.0056
		(10,10)	68.6577	58.6827	53.6017	49.4451	46.6317
	0.5	(0,0)	92.1548	78.0255	70.2862	63.8707	60.5431
		(10,10)	101.5484	86.5474	78.7241	72.2960	68.2773
$\frac{2\pi}{3}$	1×10^{-6}	(0,0)	38.1098	32.2682	29.0727	26.4265	25.0534
		(10,10)	47.6335	40.8743	37.5466	34.8389	32.7933
	0.3	(0,0)	51.3641	43.4906	39.1822	35.6138	33.7624
		(10,10)	60.4925	51.7541	47.3395	43.7332	41.2255
	0.5	(0,0)	86.1341	72.9284	65.6961	59.7016	56.5921
		(10,10)	95.4780	81.4035	74.0854	68.0759	64.2806
π	1×10^{-6}	(0,0)	28.1513	23.8365	21.4767	19.5231	18.5092
		(10,10)	37.3978	32.1774	29.6695	27.6358	25.9804
	0.3	(0,0)	45.7471	38.7348	34.8983	31.7212	30.0726
		(10,10)	54.6732	46.8115	42.8661	39.6466	37.3594
	0.5	(0,0)	81.8461	69.2981	62.4267	56.7319	53.7779
		(10,10)	91.1473	77.7332	70.7746	65.0631	61.4275
$\frac{3\pi}{2}$	1×10^{-6}	(0,0)	28.3068	23.9682	21.5957	19.6317	18.6125
		(10,10)	36.2355	31.1259	28.6338	26.6088	25.0355
	0.3	(0,0)	43.2972	36.6605	33.0298	30.0232	28.4632
		(10,10)	52.1041	44.6276	40.8870	37.8362	35.6475
	0.5	(0,0)	79.9448	67.6884	60.9771	55.4151	52.5299
		(10,10)	89.2247	76.1036	69.3044	63.7249	60.1602
2π	1×10^{-6}	(0,0)	28.6559	24.2639	21.8623	19.8742	18.8425
		(10,10)	36.1299	31.0126	28.5003	26.4569	24.9017
	0.3	(0,0)	42.4493	35.9426	32.3831	29.4355	27.9062
		(10,10)	51.2089	43.8664	40.1967	37.2044	35.0500
	0.5	(0,0)	79.2801	67.1256	60.4702	54.9547	52.0936
		(10,10)	88.5522	75.5335	68.7901	63.2567	59.7168

where dot above each parameter denotes derivative with respect to time. K_w and K_s are the Winkler and Pasternak foundation parameters, respectively. Also the resultant forces N_{rr}, $N_{\theta\theta}$ and $N_{r\theta}$ can be defined by integrating corresponding stresses along the thickness as follows

$$(N_{rr}, N_{\theta\theta}, N_{r\theta}) = \int_{-h/2}^{h/2} (\sigma_{rr}, \sigma_{\theta\theta}, \sigma_{r\theta}) \mathrm{d}z \tag{7}$$

and the resultant moments M_{rr}, $M_{\theta\theta}$ and $M_{r\theta}$ are

$$(M_{rr}, M_{\theta\theta}, M_{r\theta}) = \int_{-h/2}^{h/2} (\sigma_{rr}, \sigma_{\theta\theta}, \sigma_{r\theta}) z \mathrm{d}z \tag{8}$$

Moreover, I_0, I_1 and I_2 are the inertia terms which are defined as

$$(I_0, I_1, I_2) = \int_{-h/2}^{h/2} \rho(z)\,(1, z, z^2) \mathrm{d}z \tag{9}$$

Considering plane stress state for the FG annular sector plate, the stresses are obtained as

$$\sigma_{rr} = \frac{E(z)}{1-\nu^2}(\varepsilon_{rr} + \nu\varepsilon_{\theta\theta}) \tag{10a}$$

$$\sigma_{\theta\theta} = \frac{E(z)}{1-\nu^2}(\varepsilon_{\theta\theta} + \nu\varepsilon_{rr}) \tag{10b}$$

$$\sigma_{r\theta} = \frac{E(z)}{2(1+\nu)}(2\varepsilon_{r\theta}) \tag{10c}$$

Using equations (5), (10) and the definition of resultant forces and moments in equations (7) and (8), the following relations can be obtained

$$\begin{bmatrix} N_{rr} \\ N_{\theta\theta} \\ N_{r\theta} \\ M_{rr} \\ M_{\theta\theta} \\ M_{r\theta} \end{bmatrix} = \begin{bmatrix} A_{11} & A_{12} & 0 & B_{11} & B_{12} & 0 \\ A_{12} & A_{22} & 0 & B_{12} & B_{22} & 0 \\ 0 & 0 & A_{33} & 0 & 0 & B_{33} \\ B_{11} & B_{12} & 0 & D_{11} & D_{12} & 0 \\ B_{12} & B_{22} & 0 & D_{12} & D_{22} & 0 \\ 0 & 0 & B_{33} & 0 & 0 & D_{33} \end{bmatrix} \times \begin{bmatrix} \partial u/\partial r \\ \partial v/r\partial\theta + u/r \\ \partial u/r\partial\theta + \partial v/\partial r - v/r \\ -\partial^2 w/\partial r^2 \\ -\partial^2 w/r^2\partial\theta^2 - \partial w/r\partial r \\ -2\partial^2 w/r\partial r\partial\theta + 2\partial w/r^2\partial\theta \end{bmatrix} \tag{11}$$

where the coefficients A_{ij}, B_{ij} and D_{ij} $(i,j = 1,2,3)$ are defined as

$$\begin{aligned} (A_{11}, B_{11}, D_{11}) &= \int_{-h/2}^{h/2} \frac{E(z)}{1-\nu^2}(1, z, z^2)\mathrm{d}z \\ (A_{12}, B_{12}, D_{12}) &= \int_{-h/2}^{h/2} \frac{\nu E(z)}{1-\nu^2}(1, z, z^2)\mathrm{d}z \\ (A_{33}, B_{33}, D_{33}) &= \int_{-h/2}^{h/2} \frac{E(z)}{2(1+\nu)}(1, z, z^2)\mathrm{d}z \end{aligned} \tag{12}$$

Substituting resultant forces and moments obtained from equation (11) into equations (6), the governing equilibrium equations of motion for an FG sector plate resting on elastic foundation are obtained as

$$\begin{aligned} &A_{11}\left(\frac{\partial^2 u}{\partial r^2} + \frac{1}{r}\frac{\partial u}{\partial r} - \frac{u}{r^2} - \frac{1}{r^2}\frac{\partial v}{\partial\theta} + \frac{1}{r}\frac{\partial^2 v}{\partial r\partial\theta}\right) \\ &+ A_{33}\left(\frac{1}{r^2}\frac{\partial^2 u}{\partial\theta^2} - \frac{1}{r}\frac{\partial^2 v}{\partial r\partial\theta} - \frac{1}{r^2}\frac{\partial v}{\partial\theta}\right) \\ &+ B_{11}\left(-\frac{\partial^3 w}{\partial r^3} - \frac{1}{r}\frac{\partial^2 w}{\partial r^2} + \frac{1}{r^2}\frac{\partial w}{\partial r} + \frac{1}{r^3}\frac{\partial^2 w}{\partial\theta^2} - \frac{1}{r^2}\frac{\partial^3 w}{\partial r\partial\theta^2} + \frac{1}{r^3}\frac{\partial^2 w}{\partial\theta^2}\right) \\ &= I_0\ddot{u} - I_1\frac{\partial\ddot{w}}{\partial r} \end{aligned} \tag{13a}$$

$$\begin{aligned} &A_{11}\left(\frac{1}{r^2}\frac{\partial^2 v}{\partial\theta^2} + \frac{1}{r}\frac{\partial^2 u}{\partial r\partial\theta} + \frac{1}{r^2}\frac{\partial u}{\partial\theta}\right) \\ &+ A_{33}\left(\frac{\partial^2 v}{\partial r^2} + \frac{1}{r}\frac{\partial v}{\partial r} - \frac{v}{r^2} + \frac{1}{r^2}\frac{\partial u}{\partial\theta} - \frac{1}{r}\frac{\partial^2 u}{\partial r\partial\theta}\right) \\ &+ B_{11}\left(-\frac{1}{r}\frac{\partial^3 w}{\partial r^2\partial\theta} - \frac{1}{r^2}\frac{\partial^2 w}{\partial r\partial\theta} - \frac{1}{r^3}\frac{\partial^3 w}{\partial\theta^3}\right) \\ &= I_0\ddot{v} - I_1\frac{\partial\ddot{w}}{r\partial\theta} \end{aligned} \tag{13b}$$

$$\begin{aligned} &B_{11}\left(\frac{\partial^3 u}{\partial r^3} + \frac{2}{r}\frac{\partial^2 u}{\partial r^2} - \frac{1}{r^2}\frac{\partial u}{\partial r} + \frac{u}{r^3} + \frac{1}{r^3}\frac{\partial^2 u}{\partial\theta^2} + \frac{1}{r^2}\frac{\partial^3 u}{\partial r\partial^2\theta}\right. \\ &\left. - \frac{1}{r^2}\frac{\partial^2 v}{\partial r\partial\theta} + \frac{1}{r^3}\frac{\partial v}{\partial\theta} + \frac{1}{r^3}\frac{\partial^3 v}{\partial\theta^3} + \frac{1}{r}\frac{\partial^3 v}{\partial r^2\partial\theta}\right) \\ &- D_{11}\left(\frac{\partial^4 w}{\partial r^4} + \frac{2}{r}\frac{\partial^3 w}{\partial r^3} - \frac{1}{r^2}\frac{\partial^2 w}{\partial r^2} + \frac{1}{r^3}\frac{\partial w}{\partial r} + \frac{2}{r^2}\frac{\partial^4 w}{\partial r^2\partial\theta^2}\right. \\ &\left. - \frac{2}{r^3}\frac{\partial^3 w}{\partial r\partial\theta^2} + \frac{4}{r^4}\frac{\partial^2 w}{\partial\theta^2} + \frac{1}{r^4}\frac{\partial^4 w}{\partial\theta^4}\right) - K_w w \\ &+ K_s\left(\frac{\partial^2 w}{\partial r^2} + \frac{\partial w}{r\partial r} + \frac{\partial^2 w}{r^2\partial\theta^2}\right) = I_0\ddot{w} + I_1\left(\frac{\partial\ddot{u}}{\partial r} + \frac{\ddot{u}}{r} + \frac{1}{r}\frac{\partial\ddot{v}}{\partial\theta}\right) \\ &- I_2\left(\frac{\partial^2\ddot{w}}{\partial r^2} + \frac{\partial\ddot{w}}{r\partial r} + \frac{\partial^2\ddot{w}}{r^2\partial\theta^2}\right) \end{aligned} \tag{13c}$$

Equations (13) are three highly coupled partial differential equations in terms of in-plane and transverse displacement components. For solving such coupled equations, it is reasonable to find a method for decoupling them. Using an analytical method, three equilibrium equations (13) are decoupled. Equations (13) can be rewritten as follows

$$A_{11}\frac{\partial\varphi_1}{\partial r} + A_{33}\frac{1}{r}\frac{\partial\varphi_2}{\partial\theta} - B_{11}\frac{\partial}{\partial r}(\nabla^2 w) = I_0\ddot{u} - I_1\frac{\partial\ddot{w}}{\partial r} \tag{14a}$$

$$A_{11}\frac{1}{r}\frac{\partial\varphi_1}{\partial\theta} - A_{33}\frac{\partial\varphi_2}{\partial r} - B_{11}\frac{\partial}{r\partial\theta}(\nabla^2 w) = I_0\ddot{v} - I_1\frac{\partial\ddot{w}}{r\partial\theta} \tag{14b}$$

$$\begin{aligned} &B_{11}\nabla^2\varphi_1 - D_{11}\nabla^2\nabla^2 w - K_w w + K_s\nabla^2 w \\ &= I_0\ddot{w} + I_1\ddot{\varphi}_1 - I_2\nabla^2\ddot{w} \end{aligned} \tag{14c}$$

where ∇^2 is two dimensional Laplace operator in polar coordinates $(\nabla^2 = \partial^2/\partial r^2 + \partial/r\partial r + \partial^2/r^2\partial\theta^2)$ and the auxiliary functions φ_1 and φ_2 are defined as

$$\varphi_1 = \frac{\partial u}{\partial r} + \frac{u}{r} + \frac{1}{r}\frac{\partial v}{\partial\theta} \tag{15a}$$

$$\varphi_2 = \frac{1}{r}\frac{\partial u}{\partial\theta} - \frac{\partial v}{\partial r} - \frac{v}{r} \tag{15b}$$

Table 7. Fundamental frequency parameter $\varpi_{mk} = \omega_{mk} b^2 \sqrt{\frac{\rho_m h}{D_m}}$ of *SSCF* FG annular sector plate for some values of n, α, $\bar{K}_w$ $\bar{K}_s$ and a/b ($h/b = 0.05$)

α	a/b	$(\bar{K}_w, \bar{K}_s)$	$n = 0$	$n = 0.5$	$n = 1$	$n = 2$	$n = 5$
$\frac{\pi}{3}$	1×10^{-6}	(0,0)	24.4447	20.6968	18.6470	16.9499	16.0701
		(10,10)	37.3514	32.2847	29.9538	28.0707	26.3349
	0.3	(0,0)	26.0904	22.0902	19.9022	18.0907	17.1516
		(10,10)	38.8580	33.5584	31.0993	29.1104	27.3211
	0.5	(0,0)	36.4876	30.8921	27.8310	25.2964	23.9831
		(10,10)	48.8007	41.9798	38.6944	36.0253	33.8722
$\frac{\pi}{2}$	1×10^{-6}	(0,0)	10.5347	8.9198	8.0369	7.3062	6.9272
		(10,10)	23.5138	20.4826	19.2008	18.1725	16.9935
	0.3	(0,0)	15.6447	13.2463	11.9350	10.8496	10.2867
		(10,10)	27.6224	23.9550	22.3235	21.0080	19.6827
	0.5	(0,0)	28.9189	24.4844	22.0593	20.0518	19.0113
		(10,10)	40.3591	34.7666	32.1065	29.9474	28.1416
$\frac{2\pi}{3}$	1×10^{-6}	(0,0)	5.2836	4.4738	4.0311	3.6647	3.4746
		(10,10)	18.0980	15.8258	14.9095	14.1766	13.2368
	0.3	(0,0)	13.4764	11.4105	10.2811	9.3464	8.8616
		(10,10)	24.3052	21.0806	19.6467	18.4895	17.3234
	0.5	(0,0)	27.0944	22.9398	20.6680	18.7875	17.8129
		(10,10)	37.9150	32.6601	30.1593	28.1285	26.4338
π	1×10^{-6}	(0,0)	2.1986	1.8617	1.6775	1.5251	1.4460
		(10,10)	13.7834	12.0756	11.4038	10.8674	10.1396
	0.3	(0,0)	12.8878	10.9122	9.8323	8.9386	8.47505
		(10,10)	22.3122	19.3269	17.9801	16.8905	15.8353
	0.5	(0,0)	26.1463	22.1372	19.9451	18.1307	17.1903
		(10,10)	36.3854	31.3326	28.9203	26.9601	25.3403
$\frac{3\pi}{2}$	1×10^{-6}	(0,0)	5.4261	4.5945	4.1399	3.7638	3.5687
		(10,10)	13.1333	11.4363	10.7142	10.1333	9.4788
	0.3	(0,0)	12.9309	10.9487	9.8652	8.9686	8.5036
		(10,10)	21.5599	18.6542	17.3274	16.2523	15.2451
	0.5	(0,0)	25.8304	21.8697	19.7042	17.9119	16.9829
		(10,10)	35.7708	30.7961	28.4155	26.4804	24.8926
2π	1×10^{-6}	(0,0)	6.3426	5.3705	4.8392	4.3995	4.1715
		(10,10)	13.0668	11.3470	10.5912	9.98089	9.3477
	0.3	(0,0)	12.9910	10.9996	9.9111	9.0104	8.5431
		(10,10)	21.3189	18.4367	17.1139	16.0414	15.0506
	0.5	(0,0)	25.7358	21.7897	19.6321	17.8464	16.9208
		(10,10)	35.5657	30.6165	28.2459	26.3186	24.7418

Doing some algebraic procedures, the coupled partial differential equations (14) can be reformulated into two independent partial differential equations as

$$\hat{D}\nabla^6 w + \left(\frac{B_{11}}{A_{11}} J_1 - \frac{\hat{D} I_0}{A_{11}} - J_2\right)\nabla^4 \ddot{w} + \left(\frac{I_0 J_2}{A_{11}} - \frac{I_1 J_1}{A_{11}}\right)\nabla^2 \ddot{\ddot{w}} + I_0 \nabla^2 \ddot{w} - \frac{I_0^2}{A_{11}} \ddot{\ddot{w}} + K_w \nabla^2 w - K_s \nabla^4 w = 0 \tag{16a}$$

$$A_{33}\nabla^2 \varphi_2 - I_0 \ddot{\varphi}_2 = 0 \tag{16b}$$

where the constant parameters $\hat{D}, J_1$ and J_2 are defined as

$$\hat{D} = D_{11} - \frac{B_{11}^2}{A_{11}}$$
$$J_1 = I_1 - \frac{B_{11} I_0}{A_{11}} \tag{17}$$
$$J_2 = I_2 - \frac{B_{11} I_1}{A_{11}}$$

The first decoupled equation (16a) is a sixth order partial differential equation in terms of transverse deflection and the second one is a second order partial

Table 8. Fundamental frequency parameter $\varpi_{mk} = \omega_{mk} b^2 \sqrt{\frac{\rho_m h}{D_m}}$ of *SSFC* FG annular sector plate for some values of n, α, $\bar{K}_w$, $\bar{K}_s$ and a/b ($h/b = 0.05$)

α	a/b	$(\bar{K}_w, \bar{K}_s)$	$n = 0$	$n = 0.5$	$n = 1$	$n = 2$	$n = 5$
$\frac{\pi}{3}$	1×10^{-6}	(0,0)	99.8879	84.5733	76.1855	69.2328	65.6265
		(10,10)	108.2674	92.1786	83.7209	76.7626	72.5372
	0.3	(0,0)	96.0549	81.3286	73.2636	66.5790	63.1113
		(10,10)	104.3906	88.8937	80.7583	74.0672	69.9841
	0.5	(0,0)	89.7937	76.0257	68.4879	62.2420	59.0032
		(10,10)	97.8988	83.3796	75.7708	69.5159	65.6806
$\frac{\pi}{2}$	1×10^{-6}	(0,0)	68.3768	57.8950	52.1584	47.4062	44.9407
		(10,10)	76.4234	65.1903	59.3757	54.6067	51.5537
	0.3	(0,0)	63.9168	54.1193	48.7580	44.3174	42.0133
		(10,10)	71.4847	60.9809	55.5467	51.0908	48.2340
	0.5	(0,0)	63.0516	53.3841	48.0943	43.7133	41.4420
		(10,10)	71.3356	60.8866	55.5054	51.0953	48.2258
$\frac{2\pi}{3}$	1×10^{-6}	(0,0)	54.4381	46.0935	41.5281	37.7471	35.7853
		(10,10)	62.2487	53.1694	48.5204	44.7149	42.1876
	0.3	(0,0)	50.4790	42.7417	38.5092	35.0046	33.1861
		(10,10)	57.5363	49.1360	44.8297	41.3047	38.9745
	0.5	(0,0)	52.1750	44.1749	39.7984	36.1745	34.2958
		(10,10)	60.8895	52.0556	47.5662	43.8942	41.3959
π	1×10^{-6}	(0,0)	41.7357	35.3386	31.8397	28.9426	27.4394
		(10,10)	49.2377	42.1276	38.5384	35.6073	33.5669
	0.3	(0,0)	38.3805	32.4976	29.2804	26.6171	25.2352
		(10,10)	45.2838	38.7430	35.4403	32.7433	30.8686
	0.5	(0,0)	43.2689	36.6343	33.0052	30.0006	28.4432
		(10,10)	52.6814	45.1302	41.3570	41.3570	36.0633
$\frac{3\pi}{2}$	1×10^{-6}	(0,0)	43.3625	36.7163	33.0817	30.0728	28.5114
		(10,10)	49.2953	42.0919	38.3954	35.3696	33.3783
	0.3	(0,0)	30.9842	26.2348	23.6378	21.4882	20.3730
		(10,10)	38.3280	32.8641	30.1561	27.9495	26.3214
	0.5	(0,0)	38.7837	32.8367	29.5839	26.8910	25.4952
		(10,10)	48.7254	41.7990	38.3786	35.5906	33.5099
2π	1×10^{-6}	(0,0)	43.9405	37.2057	33.5230	30.4742	28.8922
		(10,10)	49.4084	42.1614	38.4236	35.3614	33.3820
	0.3	(0,0)	27.7008	23.4546	21.1329	19.2111	18.2143
		(10,10)	35.4578	30.4467	27.9935	25.9972	24.4663
	0.5	(0,0)	37.1017	31.4126	28.3009	25.7249	24.3897
		(10,10)	47.2813	40.5845	37.2945	34.6142	32.5813

differential equation in terms of function φ_2. It can be seen that the total order of the decoupled equations is the same as the total order of coupled equations (13).

Also, the function φ_1 can be related to the transverse deflections through the following relation

$$\ddot{\varphi}_1 = \frac{-1}{J_1}\left(\hat{D}\,\nabla^4 w - J_2\nabla^2\ddot{w} + I_0\ddot{w} + K_w w - K_s\nabla^2 w\right) \quad (18)$$

In order to apply the boundary conditions, the in-plane displacements of the annular sector plate should be expressed in terms of functions w, φ_1 and φ_2. Considering equations (13a), (13b) and (15), it is easy to show that

$$\begin{aligned}\ddot{u} &= \frac{1}{I_0}\left(A_{11}\frac{\partial\varphi_1}{\partial r} + A_{33}\frac{\partial\varphi_2}{r\partial\theta} - B_{11}\frac{\partial}{\partial r}(\nabla^2 w) + I_1\frac{\partial\ddot{w}}{\partial r}\right)\\ \ddot{v} &= \frac{1}{I_0}\left(A_{11}\frac{\partial\varphi_1}{r\partial\theta} - A_{33}\frac{\partial\varphi_2}{\partial r} - B_{11}\frac{\partial}{r\partial\theta}(\nabla^2 w) + I_1\frac{\partial\ddot{w}}{r\partial\theta}\right)\end{aligned} \quad (19)$$

It can be concluded that by solving the independent equations (16) and introducing the results into equations (18) and then substituting into equation (19), the general solutions of the FG annular sector plates can be obtained.

4. Free vibration of FG annular sector plates

For free harmonic vibration analysis of the FG annular sector plate with simply supported radial edges, the transverse displacement w and function φ_2 are represented as

$$\begin{aligned} w(r,\theta,z,t) &= \sum_{m=1}^{\infty} w_{mk}(r)\sin(\beta_m\theta)\, e^{i\omega_{mk}\, t} \\ \varphi_2(r,\theta,z,t) &= \sum_{m=1}^{\infty} \varphi_{mk}(r)\cos(\beta_m\theta)\, e^{i\omega_{mk}\, t} \end{aligned} \tag{20}$$

where β_m denotes $m\pi/\alpha$, ω_{mk}'s are the natural frequencies of the FG annular sector plate and parameters m and k denote the mode number in $\theta-$ and $r-$ directions, respectively.

Substituting the proposed series solutions (20) into equation (16), two ordinary differential equations are obtained as follows

$$\begin{aligned} &\frac{d^6 w_{mk}}{\mathrm{d}r^6} + \lambda_1 \frac{d^5 w_{mk}}{\mathrm{d}r^5} + \lambda_2 \frac{d^4 w_{mk}}{\mathrm{d}r^4} + \lambda_3 \frac{d^3 w_{mk}}{\mathrm{d}r^3} \\ &\quad + \lambda_4 \frac{d^2 w_{mk}}{\mathrm{d}r^2} + \lambda_5 \frac{dw_{mk}}{\mathrm{d}r} + \lambda_6 w_{mk} = 0 \end{aligned} \tag{21a}$$

$$\frac{d^2\varphi_{mk}}{\mathrm{d}r^2} + \frac{1}{r}\frac{d\varphi_{mk}}{\mathrm{d}r} + \left(\frac{I_0\omega_{mk}^2}{A_{33}} - \frac{\beta_m^2}{r^2}\right)\varphi_{mk}(r) = 0 \tag{21b}$$

where $\lambda_i\,(i = 1..6)$ are defined as

$$\begin{aligned} \lambda_1 &= \frac{3}{r},\ \lambda_2 = -\frac{3\beta_m^2}{r^2} - \frac{\omega_{mk}^2 B_{11} J_1}{A_{11}\hat{D}} + \frac{J_2\omega_{mk}^2}{\hat{D}} \\ &\quad + \frac{I_0\omega_{mk}^2}{A_{11}} - \frac{3}{r^2} - \frac{K_s}{\hat{D}} \\ \lambda_3 &= -\frac{2\omega_{mk}^2 B_{11} J_1}{r A_{11}\hat{D}} + \frac{2J_2\omega_{mk}^2}{r\hat{D}} + \frac{6}{r^3} - \frac{2\,K_s}{r\hat{D}} \\ &\quad + \frac{2\,\omega_{mk}^2\, I_0}{r\, A_{11}} + \frac{6\,\beta_m^2}{r^3} \\ \lambda_4 &= -\frac{9}{r^4} - \frac{21\,\beta_m^2}{r^4} + \frac{\omega_{mk}^2\, B_{11} J_1}{r^2\, A_{11}\hat{D}} + \frac{K_s}{r^2\hat{D}} - \frac{\omega_{mk}^4 I_1 J_1}{A_{11}\hat{D}} \\ &\quad - \frac{2\omega_{mk}^2\, J_2\beta_m^2}{r^2\hat{D}} + \frac{3\,\beta_m^4}{r^4} - \frac{\omega_{mk}^2\, I_0}{r^2 A_{11}} - \frac{I_0\omega_{mk}^2}{\hat{D}} \\ &\quad + \frac{2\omega_{mk}^2 B_{11} J_1\beta_m^2}{r^2 A_{11}\hat{D}} + \frac{K_w}{\hat{D}} + \frac{I_0 J_2\omega_{mk}^4}{A_{11}\hat{D}} + \frac{2K_s\beta_m^2}{r^2\hat{D}} \\ &\quad - \frac{J_2\omega_{mk}^2}{r^2\hat{D}} - \frac{2\,I_0\beta_m^2\omega_{mk}^2}{r^2 A_{11}} \\ \lambda_5 &= -\frac{2\,B_{11} J_1\beta_m^2\omega_{mk}^2}{r^3 A_{11}\hat{D}} - \frac{K_s}{r^3\hat{D}} - \frac{B_{11} J_1\omega_{mk}^2}{A_{11} r^3\hat{D}} + \frac{9}{r^5} - \frac{2\,K_s\beta_m^2}{r^3\hat{D}} \\ &\quad + \frac{2\,I_0\beta_m^2\omega_{mk}^2}{r^3 A_{11}} - \frac{I_1 J_1\omega_{mk}^4}{r A_{11}\hat{D}} + \frac{I_0\,\omega_{mk}^2}{A_{11} r^3} - \frac{I_0\omega_{mk}^2}{r\hat{D}} - \frac{9\,\beta_m^4}{r^5} \\ &\quad + \frac{I_0 J_2\omega_{mk}^4}{A_{11} r\hat{D}} + \frac{K_w}{r\hat{D}} + \frac{2\omega_{mk}^2 J_2\beta_m^2}{r^3\hat{D}} + \frac{J_2\omega_{mk}^2}{r^3\hat{D}} + \frac{45\,\beta_m^2}{r^5} \end{aligned}$$

$$\begin{aligned} \lambda_6 &= \frac{J_2\omega_{mk}^2\beta_m^4}{r^4\hat{D}} - \frac{\beta_m^6}{r^6} - \frac{K_s\beta_m^4}{r^4\hat{D}} + \frac{I_0\omega_{mk}^2\beta_m^4}{A_{11} r^4} - \frac{64\,\beta_m^2}{r^6} \\ &\quad + \frac{20\,\beta_m^4}{r^6} - \frac{I_0^2\omega_{mk}^4}{A_{11}\hat{D}} + \frac{4\,K_s\beta_m^2}{r^4\hat{D}} + \frac{I_0\omega_{mk}^2\beta_m^2}{r^2\hat{D}} + \frac{I_1 J_1\omega_{mk}^4\beta_m^2}{A_{11} r^2\hat{D}} \\ &\quad - \frac{K_w\beta_m^2}{r^2\hat{D}} - \frac{I_0 J_2\omega_{mk}^4\beta_m^2}{A_{11} r^2\hat{D}} + \frac{4\,B_{11} J_1\omega_{mk}^2\beta_m^2}{r^4 A_{11}\hat{D}} \\ &\quad - \frac{4 I_0\omega_{mk}^2\beta_m^2}{A_{11} r^4} - \frac{B_{11} J_1\omega_{mk}^2\beta_m^4}{A_{11} r^4\hat{D}} - \frac{4 J_2\omega_{mk}^2\beta_m^2}{r^4\hat{D}} \end{aligned} \tag{22}$$

The general solutions of two ordinary differential equations (21) can be expressed in terms of Bessel functions as

$$\begin{aligned} w_{mk}(r) &= C_1 J_{\beta_m}(\sqrt{\eta_1} r) + C_2\, Y_{\beta_m}(\sqrt{\eta_1} r) \\ &\quad + C_3 J_{\beta_m}(\sqrt{\eta_2} r) + C_4\, Y_{\beta_m}(\sqrt{\eta_2} r) + C_5 J_{\beta_m}(\sqrt{\eta_3} r) \\ &\quad + C_6\, Y_{\beta_m}(\sqrt{\eta_3} r) \end{aligned} \tag{23a}$$

$$\varphi_{mk}(r) = C_7 J_{\beta_m}\left(\sqrt{\frac{I_0\omega_{mk}^2}{A_{33}}}\right) + C_8\, Y_{\beta_m}\left(\sqrt{\frac{I_0\omega_{mk}^2}{A_{33}}}\right) \tag{23b}$$

where J and Y are respectively first and second Bessel functions and the parameters η_i $(i = 1..3)$ are defined as

$$\begin{aligned} \eta_1 &= -\frac{T}{6\mu_1} + \frac{2(3\mu_3\mu_1 - \mu_2^2)}{3\mu_1 T} + \frac{\mu_2}{3\mu_1} \\ \eta_2 &= \frac{T}{12\mu_1} - \frac{3\mu_3\mu_1 - \mu_2^2}{3\mu_1 T} + \frac{\mu_2}{3\mu_1} \\ &\quad - \frac{\sqrt{3}i}{2}\left(\frac{T}{6\mu_1} + \frac{2(3\mu_3\mu_1 - \mu_2^2)}{3\mu_1 T}\right) \\ \eta_3 &= \frac{T}{12\mu_1} - \frac{3\mu_3\mu_1 - \mu_2^2}{3\mu_1 T} + \frac{\mu_2}{3\mu_1} \\ &\quad + \frac{\sqrt{3}i}{2}\left(\frac{T}{6\mu_1} + \frac{2(3\mu_3\mu_1 - \mu_2^2)}{3\mu_1 T}\right) \end{aligned} \tag{24}$$

where the parameters T and μ_i $(i = 1..4)$ are defined as

$$\begin{aligned} T &= (36\mu_1\mu_3\mu_2 - 108\mu_4\mu_1^2 - 8\mu_2^3 + 12\sqrt{3}\mu_1 \\ &\quad \times \sqrt{4\mu_1\mu_3^3 - \mu_3^2\mu_2^2 - 18\mu_1\mu_3\mu_2\mu_4 + 27\mu_3^2\mu_1^2 + 4\mu_3\mu_2^3})^{\frac{1}{3}} \\ \mu_1 &= B_{11}(A_{11}D_{11} - B_{11}^2) \\ \mu_2 &= B_{11}\omega_{mk}^2(I_2 A_{11} - I_1 B_{11}) - K_s A_{11} B_{11} \\ &\quad - D_{11}\omega_{mk}^2(I_1 A_{11} - I_0 B_{11}) + I_1\omega_{mk}^2(A_{11}D_{11} - B_{11}^2) \\ \mu_3 &= (K_w - I_0\omega_{mk}^2)B_{11} A_{11} \\ &\quad + (I_1 A_{11} - I_0 B_{11})(K_s\omega_{mk}^2 - I_2\omega_{mk}^4) \\ &\quad + I_1\omega_{mk}^2((I_2 A_{11} - I_1 B_{11})\omega_{mk}^2 - K_s A_{11}) \\ \mu_4 &= I_0 B_{11}\omega_{mk}^2(K_w - I_0\omega_{mk}^2) \end{aligned} \tag{25}$$

It is noticeable that as each of parameters η_i $(i = 1, \ldots, 3)$ becomes negative in equation (24), its corresponding Bessel function in equation (23a) will convert to the modified Bessel function. Introducing the transverse displacement and function φ_2 into equations

Table 9. Fundamental frequency parameter $\varpi_{mk} = \omega_{mk} b^2 \sqrt{\frac{\rho_m h}{D_m}}$ of *SSSF* FG annular sector plate for some values of n, α, $\bar{K}_w$, $\bar{K}_s$ and a/b ($h/b = 0.05$)

α	a/b	$(\bar{K}_w, \bar{K}_s)$	$n = 0$	$n = 0.5$	$n = 1$	$n = 2$	$n = 5$
$\frac{\pi}{3}$	1×10^{-6}	(0,0)	24.4447	20.6968	18.6470	16.9499	16.0700
		(10,10)	37.3514	32.2847	29.9538	28.0707	26.3349
	0.3	(0,0)	24.7838	20.9839	18.9056	17.1850	16.2929
		(10,10)	37.7093	32.5896	30.2311	28.3254	26.5755
	0.5	(0,0)	27.5823	23.3530	21.0396	19.1242	18.1313
		(10,10)	41.0002	35.4083	32.8138	30.7158	28.8272
$\frac{\pi}{2}$	1×10^{-6}	(0,0)	10.5348	8.9199	8.0370	7.3062	6.9272
		(10,10)	23.5137	20.4826	19.2008	18.1725	16.9934
	0.3	(0,0)	11.9547	10.1221	9.1202	8.2909	7.8607
		(10,10)	24.8234	21.5989	20.2168	19.1067	17.8756
	0.5	(0,0)	15.7024	13.2950	11.9786	10.8889	10.3239
		(10,10)	29.5842	25.6992	24.0031	22.6387	21.1941
$\frac{2\pi}{3}$	1×10^{-6}	(0,0)	5.2837	4.4737	4.0311	3.6647	3.4746
		(10,10)	18.0979	15.8258	14.9095	14.1766	13.2368
	0.3	(0,0)	8.1935	6.9375	6.2509	5.6827	5.3879
		(10,10)	20.4373	17.8223	16.7302	15.8542	14.8197
	0.5	(0,0)	11.9126	10.0863	9.0878	8.2614	7.8328
		(10,10)	25.8262	22.4857	21.0643	19.9226	18.6344
π	1×10^{-6}	(0,0)	2.0853	1.7657	1.5911	1.4465	1.3715
		(10,10)	13.7574	12.0540	11.3849	10.8506	10.1236
	0.3	(0,0)	6.6351	5.6181	5.0621	4.6021	4.3635
		(10,10)	17.4608	15.2309	14.3023	13.5571	12.6716
	0.5	(0,0)	9.5616	8.0958	7.2944	6.6312	6.2873
		(10,10)	23.2807	20.2977	19.0488	18.0465	16.8704
$\frac{3\pi}{2}$	1×10^{-6}	(0,0)	5.4255	4.5939	4.1395	3.7634	3.5682
		(10,10)	13.1328	11.4359	10.7138	10.1329	9.4784
	0.3	(0,0)	6.5194	5.5201	4.9739	4.5219	4.2874
		(10,10)	16.2152	14.1335	13.2582	12.5552	11.7391
	0.5	(0,0)	8.6902	7.3580	6.6297	6.0270	5.7144
		(10,10)	22.1994	19.3639	18.1831	17.2355	16.1096
2π	1×10^{-6}	(0,0)	6.3426	5.3705	4.8392	4.3995	4.1714
		(10,10)	13.0668	11.3470	10.5912	9.9808	9.3476
	0.3	(0,0)	6.5790	5.5706	5.0195	4.5634	4.3267
		(10,10)	15.7951	13.7607	12.9004	12.2089	11.4177
	0.5	(0,0)	8.4206	7.1297	6.4240	5.8400	5.5371
		(10,10)	21.8296	19.0437	17.8853	16.9556	15.8473

(18) and (19) by help of equation (20), the in-plane displacements can be obtained.

The natural frequencies of the FG annular plate can be obtained by imposing the boundary conditions at two circular edges. Depending on specific boundary conditions, each of the edges has one of the following conditions

$$\text{Clamped:} \quad u(r,\theta) = v(r,\theta) = w(r,\theta) = \frac{\partial w(r,\theta)}{\partial r} = 0 \text{ at } r = a,\ b \tag{26a}$$

$$\text{Simply support:} \ w(r,\theta) = M_{rr}(r,\theta) = N_{rr}(r,\theta) = v(r,\theta) = 0 \text{ at } r = a,\ b \tag{26b}$$

$$\text{Free:} \ N_{rr}(r,\theta) = N_{r\theta}(r,\theta) = M_{rr}(r,\theta) = \partial M_{rr}/\partial r + 2\partial M_{r\theta}/(r\partial\theta) + (M_{rr} - M_{\theta\theta})/r + K_s \partial w/\partial r = 0 \text{ at } r = a,\ b \tag{26c}$$

where the stress and moment resultants have been defined in equation (11). Also, the in-plane

Table 10. Fundamental frequency parameter $\varpi_{mk} = \omega_{mk} b^2 \sqrt{\frac{\rho_m h}{D_m}}$ of *SSFS* FG annular sector plate for some values of n, α, $\bar{K}_w$, $\bar{K}_s$ and a/b ($h/b = 0.05$)

α	a/b	$(\bar{K}_w, \bar{K}_s)$	$n = 0$	$n = 0.5$	$n = 1$	$n = 2$	$n = 5$
$\frac{\pi}{3}$	1×10^{-6}	(0,0)	78.2450	66.2492	59.6803	54.2362	51.4122
		(10,10)	87.8753	74.9803	68.3177	62.8527	59.3250
	0.3	(0,0)	75.9328	64.2917	57.9175	52.6349	49.8946
		(10,10)	85.5359	72.9972	66.5281	61.2231	57.7818
	0.5	(0,0)	69.8381	59.1314	53.2702	48.4140	45.8949
		(10,10)	79.0432	67.4750	61.5215	56.6424	53.4526
$\frac{\pi}{2}$	1×10^{-6}	(0,0)	50.2308	42.5309	38.3174	34.8274	33.0167
		(10,10)	59.8038	51.1942	46.8653	43.3315	40.8346
	0.3	(0,0)	47.3007	40.0503	36.0832	32.7975	31.0927
		(10,10)	56.5049	48.3782	44.2980	40.9680	38.6048
	0.5	(0,0)	43.8807	37.1537	33.4733	30.4254	28.8443
		(10,10)	53.3727	45.7368	41.9329	38.8318	36.5752
$\frac{2\pi}{3}$	1×10^{-6}	(0,0)	38.1098	32.2682	29.0727	26.4265	25.0534
		(10,10)	47.6335	40.8743	37.5466	34.8389	32.7933
	0.3	(0,0)	35.5396	30.0923	27.1127	24.6456	23.3654
		(10,10)	44.3347	38.0396	34.9375	32.4132	30.5122
	0.5	(0,0)	32.8071	27.7777	25.0267	22.7489	21.5674
		(10,10)	42.9840	36.9587	34.0456	31.6804	29.7914
π	1×10^{-6}	(0,0)	27.2891	23.1063	20.8189	18.9250	17.9423
		(10,10)	36.7403	31.6290	29.1859	27.2062	25.5697
	0.3	(0,0)	25.1716	21.3136	19.2039	17.4574	16.5512
		(10,10)	33.7186	29.0218	26.7727	24.9500	23.4520
	0.5	(0,0)	22.8069	19.3106	17.3985	15.8156	14.9946
		(10,10)	34.4737	29.7939	27.6393	25.8998	24.2989
$\frac{3\pi}{2}$	1×10^{-6}	(0,0)	28.2969	23.9599	21.5882	19.6249	18.6061
		(10,10)	36.2265	31.1183	28.6269	26.6026	25.0296
	0.3	(0,0)	18.5849	15.7365	14.1790	12.8899	12.2209
		(10,10)	27.5781	23.8251	22.0916	20.6927	19.4172
	0.5	(0,0)	16.8598	14.2752	12.8618	11.6918	11.5527
		(10,10)	30.1534	26.1736	24.4227	23.0148	21.5518
2π	1×10^{-6}	(0,0)	28.6557	24.2637	21.8621	19.8740	18.8423
		(10,10)	36.1296	31.0124	28.5001	26.4567	24.9016
	0.3	(0,0)	15.3742	13.0178	11.7295	11.5527	11.5527
		(10,10)	24.9604	21.6206	20.1189	18.9104	17.7241
	0.5	(0,0)	14.2500	12.0655	10.8709	9.8820	9.3692
		(10,10)	28.5196	24.8091	23.2157	21.9368	20.5239

displacements $u(r, \theta)$ and $v(r, \theta)$ are obtained by introducing equations (18) and (20) into equation (19).

By imposing the boundary conditions along the circular edges at $r = a$ and $r = b$, eight homogeneous algebraic equations are obtained. Setting the characteristic determinant of the eight order coefficient matrix equal to zero, the natural frequencies of the FG sector plate can be evaluated.

5. Numerical results

The FG annular sector plate is simply supported at radial edges and the boundary conditions along the circular edges are identified according to the inner and outer radius of the annular sector plates (e.g. *SSCF* denotes a plate with simply supported radial edges, clamped inner and free outer circular edges). The nine

Table 11. Fundamental frequency parameter $\varpi_{mk} = \omega_{mk} b^2 \sqrt{\frac{\rho_m h}{D_m}}$ of *SSFF* FG annular sector plate for some values of n, α, $\bar{K}_w$, $\bar{K}_s$ and a/b ($h/b = 0.05$)

α	a/b	$(\bar{K}_w, \bar{K}_s)$	$n = 0$	$n = 0.5$	$n = 1$	$n = 2$	$n = 5$
$\frac{\pi}{3}$	1×10^{-6}	(0,0)	24.4447	20.6968	18.6470	16.9499	16.0700
		(10,10)	37.3514	32.2847	29.9538	28.0707	26.3349
	0.3	(0,0)	24.1040	20.4085	18.3872	16.7138	15.8462
		(10,10)	37.0292	32.0115	29.7069	27.8453	26.1216
	0.5	(0,0)	22.4517	19.0095	17.1270	15.5685	14.7603
		(10,10)	35.1818	30.4270	28.2514	26.4938	24.8500
$\frac{\pi}{2}$	1×10^{-6}	(0,0)	10.5259	8.9144	8.0306	7.3027	6.9128
		(10,10)	23.5138	20.4826	19.2008	18.1724	16.9935
	0.3	(0,0)	9.6451	8.1666	7.3583	6.6893	6.3423
		(10,10)	22.7897	19.8649	18.6373	17.6527	16.5033
	0.5	(0,0)	8.3969	7.1098	6.4061	5.8237	5.5216
		(10,10)	21.1246	18.4122	17.2710	16.3536	15.2906
$\frac{2\pi}{3}$	1×10^{-6}	(0,0)	5.2837	4.4737	4.0311	3.6647	3.4746
		(10,10)	18.0979	15.8258	14.9095	14.1766	13.2368
	0.3	(0,0)	4.1116	3.4814	3.1369	2.8518	2.7039
		(10,10)	17.2324	15.0769	14.2126	13.5206	12.6223
	0.5	(0,0)	3.4120	2.8891	2.6032	2.3666	2.2439
		(10,10)	15.7828	13.7956	12.9876	12.3388	11.5242
π	1×10^{-6}	(0,0)	0	0	0	0	0
		(10,10)	13.5289	11.8649	11.2199	10.7056	9.9847
	0.3	(0,0)	0	0	0	0	0
		(10,10)	12.6428	11.0726	10.4507	9.9526	9.2885
	0.5	(0,0)	0	0	0	0	0
		(10,10)	11.3727	9.9509	9.3809	8.9244	8.3318
$\frac{3\pi}{2}$	1×10^{-6}	(0,0)	5.4224	4.5913	4.1371	3.7612	3.5662
		(10,10)	13.1299	11.4334	10.7116	10.1309	9.4765
	0.3	(0,0)	1.6577	1.4036	1.2647	1.1499	1.0903
		(10,10)	9.9318	8.6877	8.1875	7.7870	7.2704
	0.5	(0,0)	1.2025	1.0182	0.9175	0.8341	0.7909
		(10,10)	8.9003	7.7901	7.3480	6.8514	6.4905
2π	1×10^{-6}	(0,0)	6.3425	5.3704	4.8392	4.3995	4.1714
		(10,10)	13.0667	11.3469	10.5912	9.9808	9.3476
	0.3	(0,0)	2.0070	1.6994	1.5313	1.3923	1.3200
		(10,10)	8.6425	7.5576	7.1204	6.7709	6.3221
	0.5	(0,0)	1.3852	1.1729	1.0568	0.9608	0.9110
		(10,10)	7.8508	6.8756	6.4907	6.1840	5.7704

possible boundary conditions containing *SSSS, SSCC, SSFF, SSCF, SSFC, SSCS, SSSC, SSSF* and *SSFS* are considered for obtaining the numerical results.

A comparison study is performed with the results reported by McGee et al. (1995) and Zhou et al. (2009) to verify the accuracy of the formulations. To this end, the annular sector plate is assumed to be homogeneous (i.e. $n = 0$). It can be seen from Table 1 that the non-dimensional frequencies are accurate. Also for some boundary conditions, the results have been compared with the results obtained from ANSYS software in Table 2 for $b = 1\,m$, $h = 0.05\,m$, $\bar{K}_w = 0$, $\bar{K}_s = 0$. To this end, the annular sector plate has been modeled in ANSYS software with tetrahedral elements type SOLID186. The comparisons have been done for three different sector angles 90°, 180°, 270°and 2 different radii ratios $a/b = 0.3$ and $a/b = 0.5$. For $a/b = 0.3$, the total numbers of elements are 10937, 11714, 15255 for the annular sector plates with sector angles 90°, 180° and 270° respectively. Also for $a/b = 0.5$, the

Table 12. Fundamental frequency parameter $\varpi_{mk} = \omega_{mk} b^2 \sqrt{\frac{\rho_m h}{D_m}}$ of FG annular sector plate for study the effect of rotary inertia (RI) ($\alpha = 60^\circ$, $h/b = 0.03$, $a/b = 0.5$)

	$(\bar{K}_w, \bar{K}_s)$		$n = 0$	$n = 0.5$	$n = 1$	$n = 2$
SSSS	(0,0)	With RI	109.8098	92.9781	83.7704	76.1457
		Without RI	110.0389	93.1697	83.9451	76.3081
	(100,100)	With RI	184.0676	159.5826	148.6723	139.8956
		Without RI	184.4513	159.9113	148.9821	140.1939
SSCC	(0,0)	With RI	193.8921	164.2111	147.9669	134.5156
		Without RI	194.3626	164.6047	148.3259	134.8496
	(100,100)	With RI	250.2917	215.1141	197.9903	184.0744
		Without RI	250.8887	215.6203	198.4611	184.5216
SSFF	(0,0)	With RI	22.4414	19.0064	17.1281	15.5738
		Without RI	22.4474	19.0114	17.1326	15.5781
	(100,100)	With RI	85.1150	74.4840	70.2317	66.8419
		Without RI	85.1555	74.5193	70.2657	66.8754
SSSC	(0,0)	With RI	153.3894	129.8773	117.0136	106.3605
		Without RI	153.7459	130.1754	117.2855	106.6133
	(100,100)	With RI	218.0785	188.0956	174.0087	162.6061
		Without RI	218.5759	188.5190	174.4045	162.9839
SSCS	(0,0)	With RI	139.5128	118.1278	106.4282	96.7391
		Without RI	139.8313	118.3942	106.6711	96.9650
	(100,100)	With RI	207.5629	179.3033	166.2261	155.6589
		Without RI	208.0283	179.7000	166.5978	156.0146
SSFS	(0,0)	With RI	69.9912	59.2636	53.3973	48.5410
		Without RI	70.0778	59.3360	53.4634	48.6025
	(100,100)	With RI	136.5988	118.8253	111.1978	105.0858
		Without RI	136.7696	118.9721	111.3369	105.2205
SSSF	(0,0)	With RI	27.5933	23.3638	21.0515	19.1379
		Without RI	27.5995	23.3689	21.0563	19.1423
	(100,100)	With RI	96.8159	84.6696	79.7825	75.8807
		Without RI	96.8645	84.7123	79.8240	75.9219
SSCF	(0,0)	With RI	36.4969	30.9024	27.8439	25.3125
		Without RI	36.5022	30.9068	27.8479	25.3162
	(100,100)	With RI	59.2706	51.4196	47.9546	45.1765
		Without RI	59.2817	51.4292	47.9637	45.1853
SSFC	(0,0)	With RI	89.9829	76.1905	68.6479	62.4038
		Without RI	90.0900	76.2800	68.7296	62.4798
	(100,100)	With RI	151.8206	131.5984	122.5650	115.2927
		Without RI	152.0122	131.7627	122.7204	115.4426

total numbers of elements are 8930, 10315, 12315 for sector angles 90°, 180° and 270°, respectively. Also, two elements are used in $z-$direction for all cases. All nodes on simply supported radial edges have been constrained in $r-$ and $z-$ directions and they are moveable in $\theta-$ direction. It can be seen that the natural frequencies are in good agreement with those obtained from an FEM commercial program based on the 3-D elasticity theory and the differences between the results are not more than 3%.

For general purposes, the non-dimensional parameters are used for numerical results as follows

$$\varpi_{mk} = \omega_{mk} b^2 \sqrt{\frac{\rho_m h}{D_m}}, \bar{K}_s = \frac{K_s b^2}{D_{11}}, \bar{K}_w = \frac{K_w b^4}{D_{11}} \qquad (27)$$

where $D_m = \frac{E_m h^3}{12(1-\nu^2)}$.

Numerical calculations have been performed for FG annular sector plates with all possible nine boundary

Table 13. Fundamental frequency parameter $\varpi_{mk} = \omega_{mk} b^2 \sqrt{\frac{\rho_m h}{D_m}}$ of FG annular sector plate for study the effect of in-plane displacements (u, v) ($h/b = 0.03$, $\alpha = 60^\circ$)

	a/b	($\bar{K}_w$, $\bar{K}_s$)		$n=0$	$n=1$	$n=2$	$n=3$	$n=4$	$n=5$
SSCC	0.3	(0,0)	with u, v	117.8503	89.9067	81.7262	79.1454	78.1014	77.4815
			without u, v	117.8503	98.0046	93.6591	91.2001	89.1467	87.3017
			difference (%)	0	−9.007	−14.601	−15.231	−14.142	−12.674
		(100,100)	with u, v	179.0546	143.6235	134.6177	130.8105	128.3198	127.5612
			without u, v	179.0546	148.9023	142.3002	138.5643	135.4445	132.6412
			Difference (%)	0	−3.675	−5.707	−5.928	−5.552	−3.982
	0.7	(0,0)	with u, v	499.5557	380.9870	346.1854	335.1934	330.7562	328.1358
			without u, v	499.5557	415.4319	396.9763	386.5351	377.8236	370.0005
			difference (%)	0	−9.041	−14.672	−15.317	−14.230	−12.758
		(100,100)	with u, v	553.6409	429.5080	394.5938	382.5423	376.6567	372.5850
			without u, v	553.6409	460.4092	439.9560	428.3847	418.7301	410.0601
			difference (%)	0	−7.194	−11.495	−11.983	−11.170	−10.058
SSSC	0.3	(0,0)	with u, v	107.2033	81.7844	74.3431	71.9955	71.0459	70.4819
			without u, v	107.2033	89.1506	85.1977	82.9609	81.0930	79.4147
			difference (%)	0	−9.006	−14.600	−15.230	−14.142	−12.674
		(100,100)	with u, v	171.6794	138.2033	129.7983	126.1546	123.7060	121.6803
			without u, v	171.6794	142.7691	136.4389	132.8569	129.8656	127.1778
			difference (%)	0	−3.304	−5.116	−5.313	−4.979	−4.518
	0.7	(0,0)	with u, v	360.9943	275.3206	250.1798	242.2400	239.0344	237.1403
			without u, v	360.9943	300.2038	286.8695	279.3256	273.0308	267.3778
			difference (%)	0	−9.037	−14.665	−15.309	−14.222	−12.751
		(100,100)	with u, v	428.7272	335.7474	310.2563	300.9791	296.0159	292.3711
			without u, v	428.7272	356.5307	340.6949	331.7357	324.2600	317.5463
			difference (%)	0	−6.190	−9.810	−10.219	−9.541	−8.610

conditions along the circular edges. For this analysis, the ceramic and metal materials have been assumed to be Alumina and Aluminum, respectively with the following properties

$$E_c = 380\,GPa, \rho_c = 3800\,Kg/m^3$$
$$E_m = 70\,GPa, \rho_m = 2707\,Kg/m^3 \quad (28)$$

Also, the Poisson ratio of the plate is assumed to be constant through the thickness and equal to 0.3. The first non-dimensional frequency parameter is shown for all possible boundary conditions along the circular edges in Tables 3 to 11 for aspect ratios 1×10^{-6} (solid sector plate), 0.3 and 0.5, different powers of FGM and for over a range of sector angles. Also, the results in tables are obtained for both the FG sector plate without elastic foundation and FG sector plate resting on Winkler and Pasternak elastic foundations.

The effect of material properties on the frequency parameter of FG annular sector plates with a specific boundary condition along the circular edges can be considered by keeping the sector angle and aspect ratio constant while varying the power of FGM. It can be seen that by increasing the power of FGM causes the non-dimensional natural frequency decreases. This is because the stiffness of the FG annular sector plates becomes lower as the power of FGM increases.

It is observed that the non-dimensional frequency increases as the aspect ratio increases except for the annular sector plates with free edges. With approaching two circular edges to each other, the stiffness of the annular sector plate increases. However, when the inner circular edge of the annular sector plate is free, the free edge get longer while the inner edge approaches to outer one and causes decreasing the frequency. In the case of *SSFC*, the variation of the frequency with respect to aspect ratio is not entirely ascendant and for some values of the aspect ratio it will increase with increasing the aspect ratio.

Also, it can be seen that for constant power of FGM and aspect ratio, the frequency parameter decreases as the sector angle α increases. The reason is that with increasing sector angle, the circumferential distance between the radial supports increases so that the stiffness of the plate decreases.

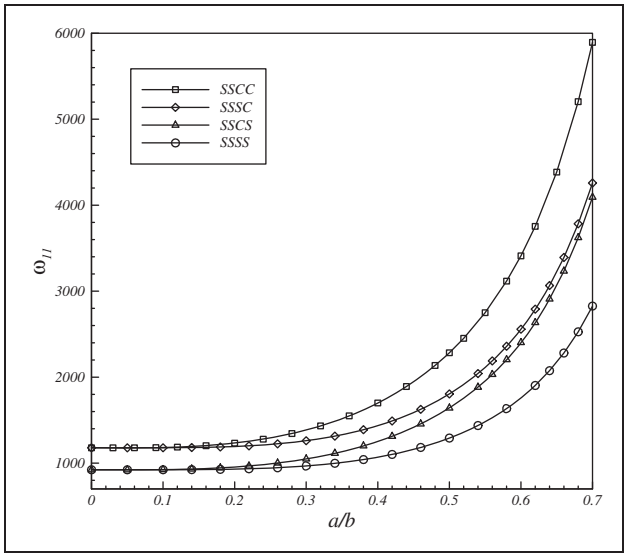

Figure 2. Variation of first natural frequency of FG annular sector plate versus the aspect ratio for various boundary conditions ($n = 1, h/b = 0.01, \alpha = 60^{\circ}$).

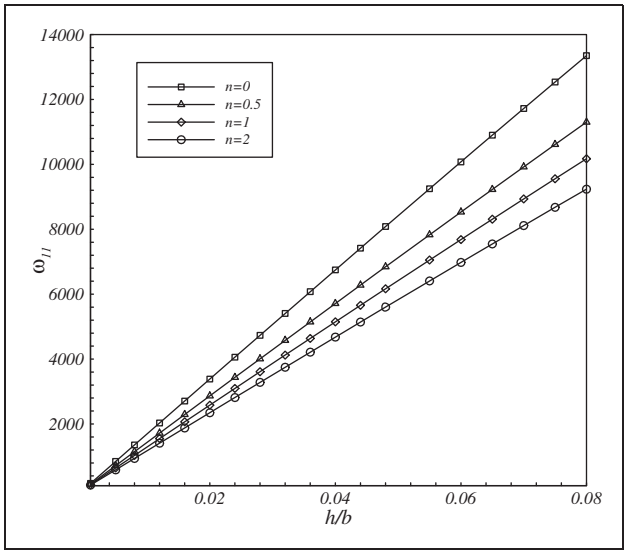

Figure 4. Variation of first natural frequency of FG annular sector plate versus the thickness-radius ratio and power law index for *SSSS* boundary condition ($a/b = 0.5, \alpha = 60^{\circ}$).

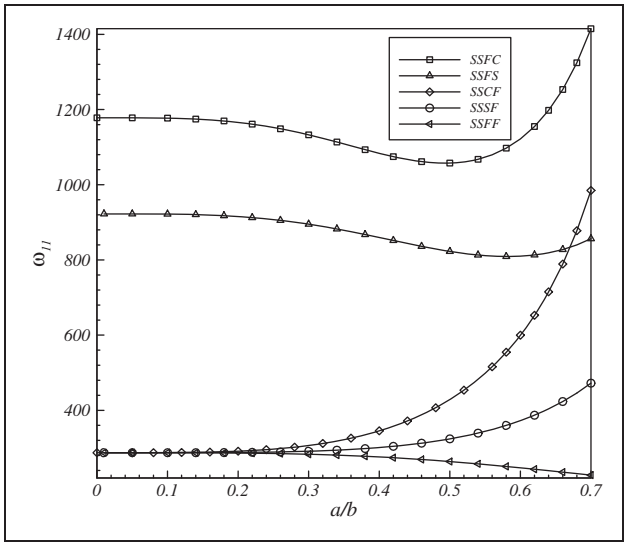

Figure 3. Variation of first natural frequency of FG annular sector plate versus the aspect ratio for boundary conditions contain free ($n = 1, h/b = 0.01, \alpha = 60^{\circ}$).

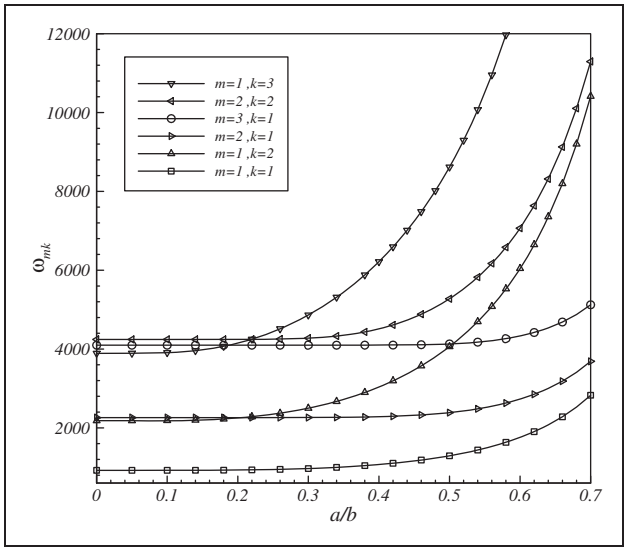

Figure 5. Variation of natural frequencies of FG annular sector plate versus the aspect ratio for *SSSS* boundary condition ($n = 1, \alpha = 60$, $h/b = 0.01$).

Besides, it can be found from Table 11 that for annular sector plate without elastic foundation with free inner and outer edges, the frequency parameter increases as the sector angle of re-entrant plate (sector plate with $\alpha > \pi$) increases. This is expected since the fundamental frequency of the semicircular plate ($\alpha = \pi$) is zero, which corresponds to a rigid body rotation of the plate about its simply supported diameter. It can be said that as the sector angle approaches 2π, the annular sector plate becomes as a complete annular plate with a hinged crack. It is expected that the natural frequencies of the annular sector plate with sector angle 2π be higher than that of axisymmetric annular plate because of the presence of a hinged crack.

Focusing on Tables 3 to 11 it can be concluded that the stiffer constrains at circular edges increase

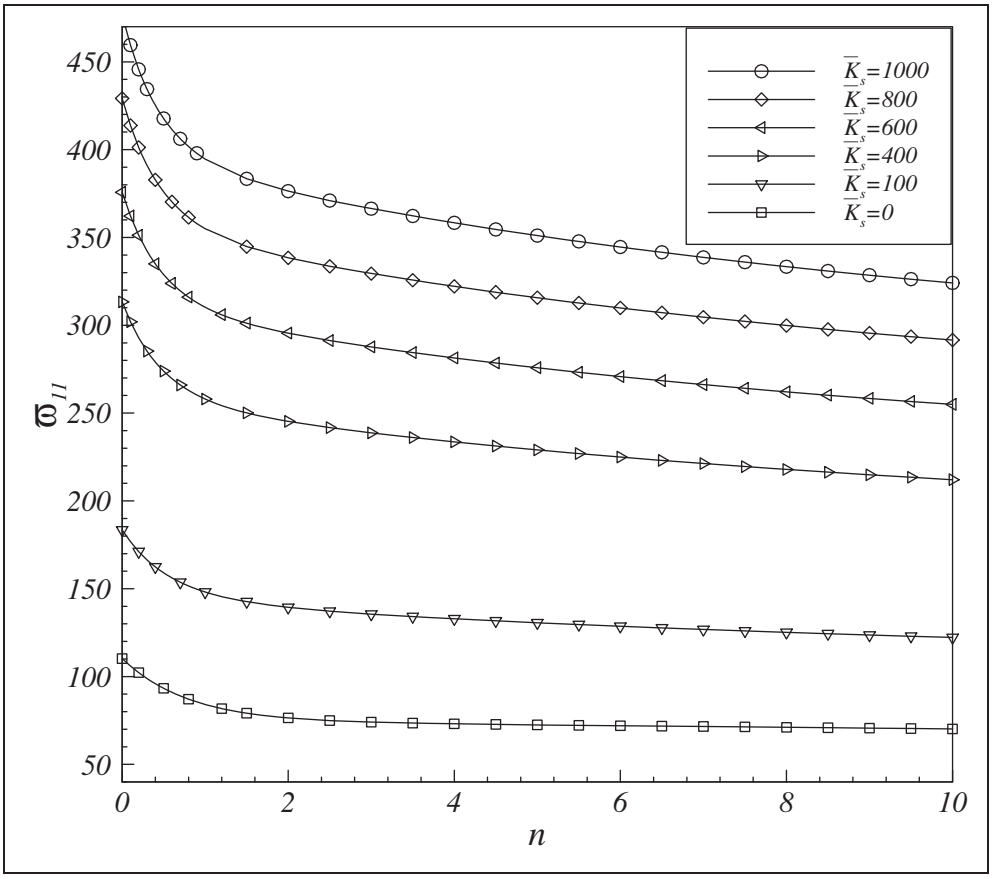

Figure 6. Variation of fundamental frequency parameter of FG annular sector plate versus the power law index and Pasternak parameter for SSSS boundary condition ($\bar{K}_w = 10$, $\alpha = 60$, $a/b = 0.5$, $h/b = 0.01$).

non-dimensional frequency of the FG annular sector plate. Therefore, the *SSCC* annular sector plate has the highest and *SSFF* annular sector plate has the lowest natural frequencies.

Yet, in the all tables the rotary inertia has been considered. In order to study the effect of rotary inertia on the natural frequencies of FG annular sector plates, the non-dimensional natural frequencies are listed in Table 12 for an FG annular sector plate with and without considering the rotary inertia. It can be seen that for all boundary conditions, neglecting the effect of rotary inertia causes the natural frequency increases. Also, this effect is valid for plates with elastic foundations. It can be concluded that the effect of rotary inertia for a plate with free edge is less than that with simply supported or clamped edges.

For studying the effect of in-plane displacements on the natural frequency of FG annular sector plates presented in Table 13. It is evident that, by increasing the power law index, the difference between the results increases. Also, for the plate under elastic foundations this effect is minor.

Based on the results presented in Table 13, it can be seen that the maximum differences have about -15.4% and this difference is not acceptable. Indeed, the in-plane displacements cause a drastic change of frequencies. In other words, neglecting the in-plane displacement for FG plate is not proper for FG plates.

This effect is more clarified in Figures 2 and 3 where the natural frequency of FG annular sector plate is depicted versus the aspect ratio for different boundary conditions. It can be seen that, the stiffness of the *SSCF* gets higher than *SSFS*. It can be seen for sector plates with free inner and outer edges, the natural frequencies decreases as the aspect ratio decreases.

To study the effect of thickness-radius ratio, the natural frequency is shown in Figure 4 versus the variation of h/b for different powers of FGM. It can be seen that the variation of natural frequencies is nearly linear with respect to thickness-radius ratio.

The influence of different mode number on the frequency of the FG sector plates is shown in Figure 5.

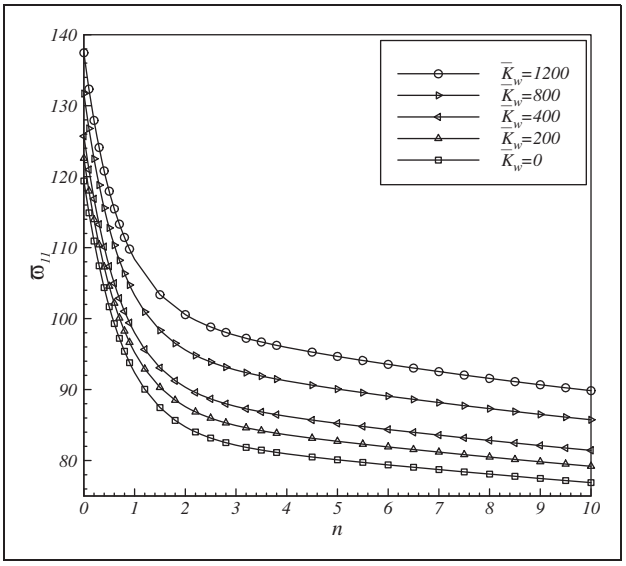

Figure 7. Variation of fundamental frequency parameter of FG annular sector plate versus the power law index and Winkler parameter for *SSSS* boundary condition ($\bar{K}_s = 10$, $\alpha = 60$, $a/b = 0.5$, $h/b = 0.01$).

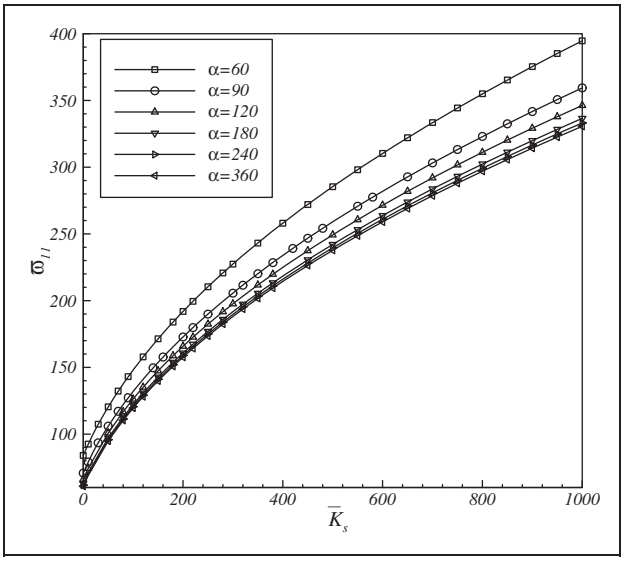

Figure 8. Variation of fundamental frequency parameter of FG annular sector plate versus the Pasternak parameter and sector angle for *SSSS* boundary condition ($K_w = 10$, $a/b = 0.5$, $h/b = 0.01$).

It can be seen that the lowest frequency is always belong to the first mode in both r and θ directions. However, the second or third mode will change by variation of aspect ratio (a/b).

The effects of elastic foundations on the natural frequencies of FG annular sector plates are shown in Figures 6, 7 and 8. It can be seen from Figure 6 that by increasing the Pasternak elastic foundation parameter, the natural frequency increases for all values of powers of FGM and changes of natural frequency become more considerable.

Figure 7 presents the variation of natural frequency versus the power law index for various values of Winkler elastic foundation parameters. It is evident that by increasing the power law index, the natural frequency decreases. By increasing the Winkler parameter the change of natural frequency is in a constant form and only the value of natural frequency increases slightly. Besides, by comparing Figures 6 and 7, it can be seen that the effect of changing the Pasternak elastic foundation parameter on the natural frequency of the sector plate is higher than that of Winkler foundation.

Natural frequency of the FG annular sector plate is depicted versus the Pasternak elastic foundation parameter in Figure 8 for different values of sector angle. It can be seen that by increasing the Pasternak parameter, the natural frequency increases for all values of sector angle. It can be seen that change of the Pasternak elastic foundation parameter has negligible effect with respect to the change of the sector angle when a sector plate with $\alpha > 180^{\circ}$.

6. Conclusion

The free vibration analysis of FG annular sector plates on elastic foundations has been considered in the present paper. The governing equations of motion have been converted into two decoupled equations. Numerical results have been compared with the existing exact solution for homogenous isotropic annular sector plate and a good agreement has been seen. Accurate frequency parameter for FG annular sector plates on Winkler and Pasternak elastic foundations has been presented for different boundary conditions along circular edges and some powers of FGM for over a wide range of sector angles. The effects of boundary conditions, powers of FGM, elastic foundation stiffness, sector angles, thickness-radius and aspect ratios on the frequency values are examined and discussed in detail. The following conclusions can be remarked:

1. The natural frequency of FG annular sector plate decreases by increases of power law index (n).
2. By increasing the aspect ratio, the natural frequency of the FG annular sector plate increases except for the boundary condition with free inner radius edge.
3. For the FG annular sector plates with *SSFC* and *SSFS* boundary conditions when $\alpha > 120^{\circ}$,

increasing the aspect ratio causes the natural frequency of FG annular sector plate first decreases and then increases. However for *SSFS* this behavior occurs for a plate on elastic foundation.
4. By increasing the sector angle, the natural frequency of the FG annular sector plate for all boundary conditions decreases.
5. For the nearly sector plate (annular sector plate with small inner edge), the effect of the inner edge condition on the natural frequency is not considerable.
6. The higher mode number changes due to the variation of the aspect ratio.
7. By increasing the elastic foundation parameter, the natural frequency of the FG sector plate increases.
8. The effect of Pasternak parameter on the natural frequency is more significant than the Winkler parameter.

Funding

This research received no specific grant from any funding agency in the public, commercial, or not-for-profit sectors.

References

Cheung YK and Kwok WL (1975) Dynamic analysis of circular and sector thick, layered plates. *Journal of Sound and Vibration* 42(2): 147–158.

Civalek O (2007) Nonlinear analysis of thin rectangular plates on Winkler–Pasternak elastic foundations by DSC–HDQ methods. *Applied Mathematical Modelling* 31: 606–624.

Harik LE and Molaghasemi HR (1990) Vibration of sector plates on elastic foundations. *Journal of Sound and Vibration* 138(3): 524–528.

Hasani Baferani A, Saidi AR and Jomehzadeh E (2011) An Exact solution for free vibration of thin functionally graded rectangular plates. *Journal of Mechanical Engineering Science,* Part: C, IMechE, 225: 526–536.

Hosseini-Hashemi S, Akhavan H, Rokni Damavandi Taher H, Daemi N and Alibeigloo A (2010a) Differential quadrature analysis of functionally graded circular and annular sector plates on elastic foundation. *Materials and Design* 31: 1871–1880.

Hosseini-Hashemi S, Rokni Damavandi Taher H and Akhavan H (2010b) Vibration analysis of radially FGM sectorial plates of variable thickness on elastic foundations. *Composite Structures* 92: 1734–1743.

Huang CS and Ho KH (2004) An analytical solution for vibrations of a polarly orthotropic Mindlin sectorial plate with simply supported radial edges. *Journal of Sound and Vibration* 273: 277–294.

Huang CS, Chang MJ and Leissa AW (2006) Vibrations of Mindlin sectorial plates using the Ritz method considering stress singularities. *Journal of Vibration and Control* 12(6): 635–657.

Huang CS, McGee OG and Leissa AW (1994) Exact analytical solutions for free vibrations of thick sectorial plates with simply supported radial edges. *International Journal of Solids and Structures* 31(11): 1609–1631.

Jomehzadeh E and Saidi AR (2009a) Analytical solution for free vibration of transversely isotropic sector plates using a boundary layer function. *Thin-Walled Structures* 47: 82–88.

Jomehzadeh E and Saidi AR (2009b) Accurate natural frequencies of transversely isotropic moderately thick annular sector plates. *Journal of Mechanical Engineering Science* Part: C, IMechE 223: 307–317.

Kim CS and Dickinson SM (1989) On the free, transverse vibration of annular and circular, thin, sectorial plates subject to certain complicating effects. *Journal of Sound and Vibration* 134(3): 407–421.

Malekzadeh P (2009) Three-dimensional free vibration analysis of thick laminated annular sector plates using a hybrid method. *Composite Structures* 90: 428–437.

Malekzadeh P, Afsari A, Zahedinejad P and Bahadori R (2010a) Three-dimensional layer wise-finite element free vibration analysis of thick laminated annular plates on elastic foundation. *Applied Mathematical Modeling* 34: 776–790.

Malekzadeh P, Golbahar Haghighi MR and Gholami M (2010b) Dynamic response of thick laminated annular sector plates subjected to moving load. *Composite Structures* 92: 155–163.

McGee OG, Huang CS and Leissa AW (1995) Comprehensive exact solutions for free vibrations of thick annular sectorial plates with simply supported radial edges. *International Journal of Mechanical Science* 37(5): 537–566.

McGee OG, Leissa AW and Huang CS (1993) vibration of completely free sectorial plates. *Journal of Sound and Vibration* 164(3): 565–569.

Mizusawa T (1991) Vibration of stepped annular sector plates by the spline element method. *Computers and Structures* 41(2): 377–383.

Nie GJ and Zhong Z (2008) Vibration analysis of functionally graded annular sectorial plates with simply supported radial edges. *Computers and Structures* 84: 167–176.

Pasternak PL (1954) *On a New Method of Analysis of an Elastic Foundation by Means of Two Foundation Constants* (in Russian). Moscow, USSR: Gosudarstrennoe Izdatelstvo Literaturi po Stroitelstvu i Arkhitekture.

Seok J and Tiersten HF (2004a) Free vibrations of annular sector cantilever plates. Part 1: out-of-plane motion. *Journal of Sound and Vibration* 271: 757–772.

Seok J and Tiersten HF (2004b) Free vibrations of annular sector cantilever plates. Part 2: in-plane motion. *Journal of Sound and Vibration* 271: 773–787.

Shiota I and Miyamoto Y (1997) *Functionally Graded Materials* 1996. Amsterdam, Elsevier.

Srinivasan RS and Thiruvekatachari V (1986) Free vibration analysis of laminated annular sector plates. *Journal of Sound and Vibration* 109(1): 89–96.

Wang X and Wang Y (2004) Free vibration analyses of thin sector plates by the new version of differential quadrature

method. *Computer Methods in Applied Mechanics and Engineering* 193: 3957–3971.

Winkler E (1867) *Die Lehre von der Elasticitaet und Festigkeit*. Prague Dominicus.

Xiang Y, Liew KM and Kitipornchai S (1993) Transverse vibration of thick annular sector plates. *ASCE Journal of Engineering Mechanics* 119(8): 1579–1599.

Yongqiang L and Jian L (2007) Free vibration analysis of circular and annular sectorial thin plates using curve strip Fourier p-element. *Journal of Sound and Vibration* 305: 457–466.

Zhou D, Lo SH and Cheung YK (2009) 3-D vibration analysis of annular sector plates using the Chebyshev–Ritz method. *Journal of Sound and Vibration* 320: 421–437.